UMassAmherst
The Commonwealth's Flagship Campus

Collective and Extrinsic Effects on Transport in 2D Materials

Zlatan Aksamija
Department of Electrical and Computer Engineering
University of Massachusetts Amherst
zlatana@engin.umass.edu

NEΘ lab

http://netlab.umasscreate.net

Materials of Interest

3

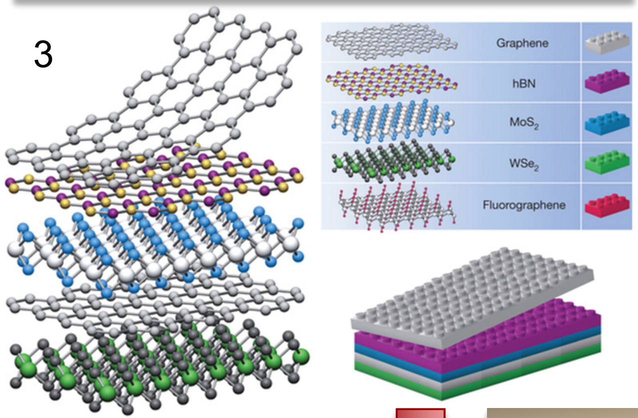

Size-dependence

1

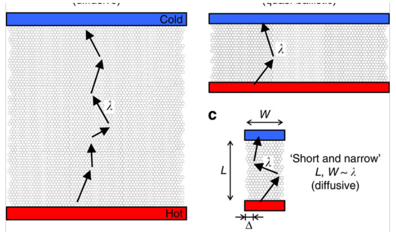

Temperature-dependence

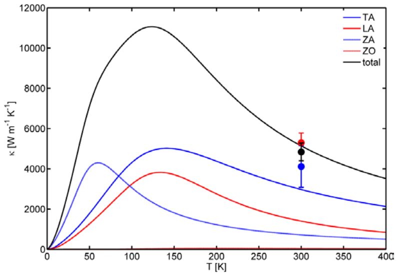

Steady-state thermal conductivity is well studied

1. Bae et al., Nat. Commun. 4, 1734, 2013.
2. Z. Aksamija and I. Knezevic, APL v.98, 141919 (2011)
3. A.K. Geim and I.V. Grigorieva, Nature 499, 419-425,2013.

2D device applications

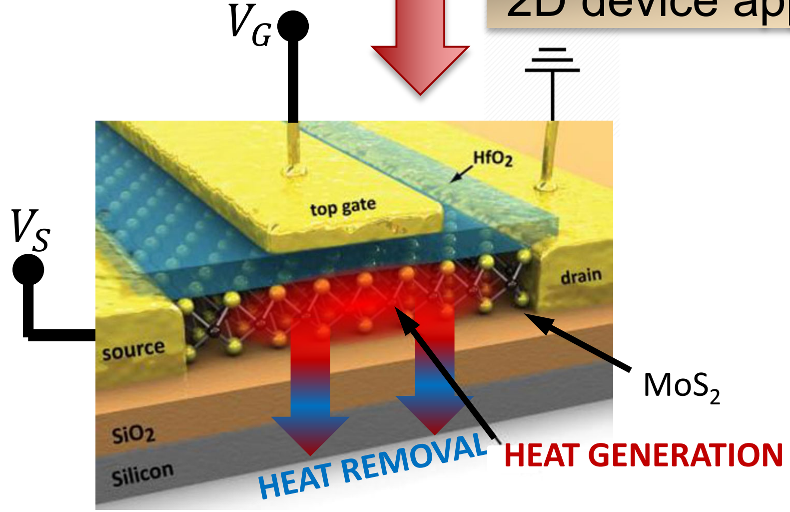

high-frequency applications

GHz applications

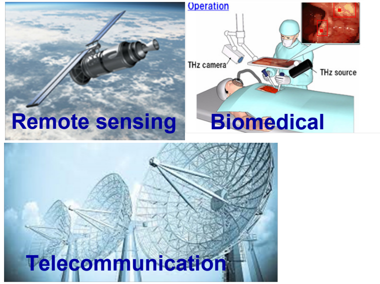

THz applications

Motivation

Effective platform for studying hydrodynamic transport and second sound

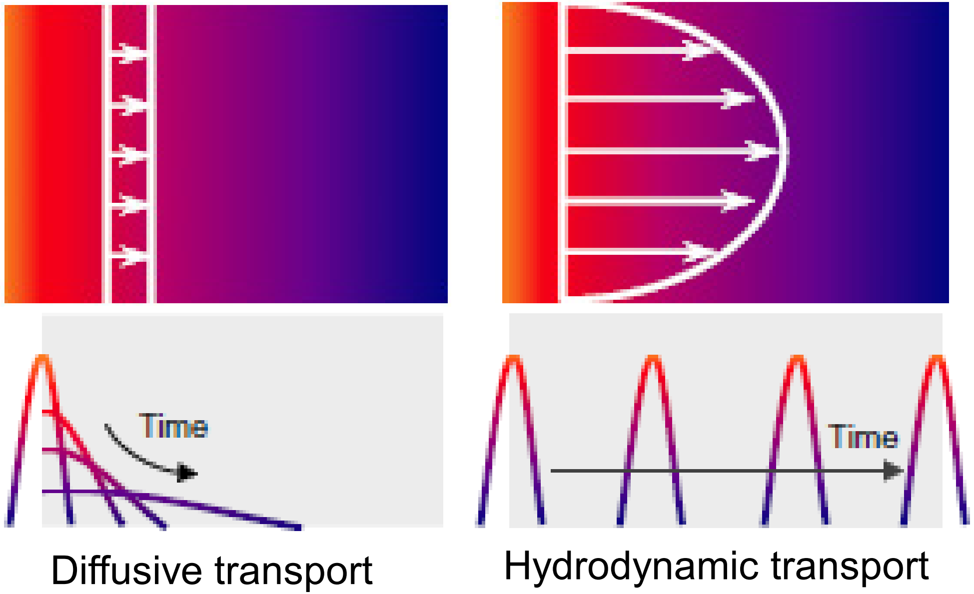

Lee et al., Nat. Commun. 6, 6290, 2015.

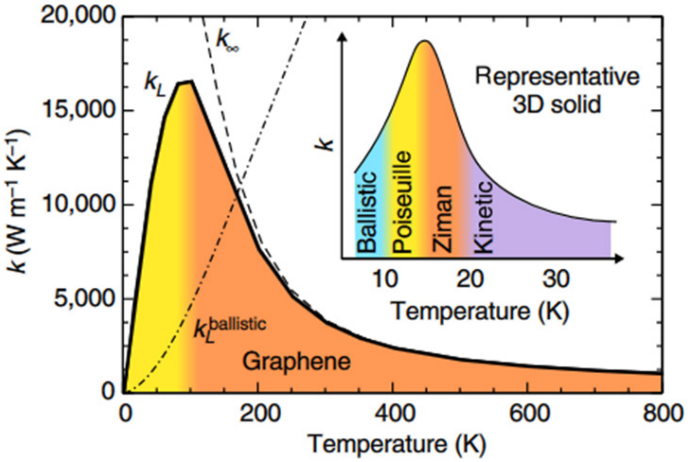

Poiseuille/Ziman regime: phonons act as a gas in a pipe

Cepellotti et al., Nat. Commun. 6, 6400, 2015.

Methodology

UMassAmherst

Phonon dispersion calculated from first-principles using Quantum Espresso

Goes into the phonon- Boltzmann Transport Equation (BTE)

$$\frac{\partial \mathrm{n_{q,b}}}{\partial t} + \mathrm{v_{q,b}} . \nabla \mathrm{n_{q,b}} = -\left(\frac{\partial \mathrm{n_{q,b}}}{\partial t}\right)_{\mathrm{collision}}$$

Using Callaway's idea

$$\left(\frac{\mathrm{n_{q,b}} - n_{q0}}{\tau_R}\right) + \left(\frac{\mathrm{n_{q,b}} - n^*_{q0}}{\tau_N}\right)$$

$$n_{q0} = \left(e^{\hbar\omega_q/K_BT} - 1\right)^{-1}, \quad n^*_{q0} = \left(e^{(\hbar\omega_q/K_BT)+\vec{\Lambda}.\vec{q}} - 1\right)^{-1}$$

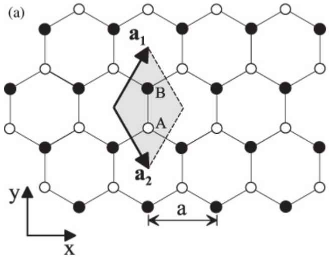

Lattice structure of graphene [4]

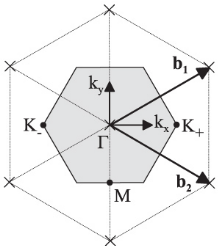

1st Brillouin zone. [4]

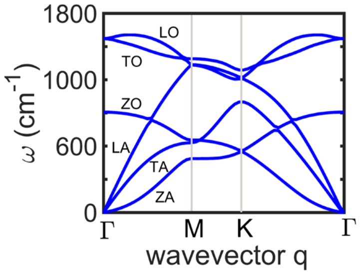

Phonon dispersion of graphene

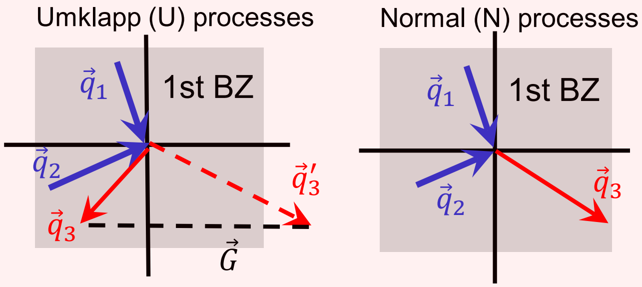

$$\frac{1}{\tau_C} = \frac{1}{\tau_R} + \frac{1}{\tau_N}$$

τ_R is the average phonon lifetime due to momentum-destroying processes:

1. Umklapp processes
2. Impurity and isotope.
3. Boundaries.

τ_N represents the average phonon lifetime due to momentum-conserving normal processes

4. E. McCann and M. Koshino, Rep. Prog. Phys. 76, 5, 2013

Phonon transport with edge roughness

- Model using the steady-state phonon Boltzmann transport equation

$$\vec{v}_{\vec{q}} \cdot \nabla_{\vec{r}} T \frac{\partial N^0_{\vec{q}}(T)}{\partial T} + v_\perp(\vec{q}) \frac{\partial n_{\vec{q}}(y)}{\partial y} = \frac{n_{\vec{q}}(y)}{\tau_{int.}(\vec{q})}$$

- In the absence of boundaries, RTA solution: $R_{\vec{q}} = \tau_{int.}(\vec{q}) \vec{v}_{\vec{q}} \cdot \nabla_{\vec{r}} T \frac{\partial N^0_{\vec{q}}(T)}{\partial T}$

- Each boundary contributes one term:

$$p(\vec{q}) \exp\left[-W/\Lambda^\perp_{int.}(\vec{q})\right]$$

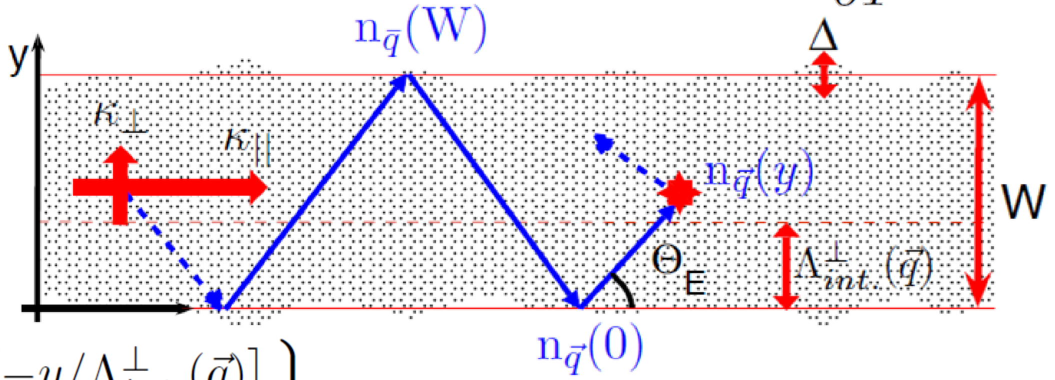

- Sum the infinite series:

$$n^+_{\vec{q}}(y) = R_{\vec{q}} \left\{ 1 - \frac{[1 - p(\vec{q})] \exp\left[-y/\Lambda^\perp_{int.}(\vec{q})\right]}{1 - p(\vec{q}) \exp\left[-W/\Lambda^\perp_{int.}(\vec{q})\right]} \right\}$$

- Heat flux weaker near edges due to roughness scattering

Position Dependence of Thermal Conductivity

Heat flux (resolved by position "y")

$$\vec{Q}^{+}(y) = \hbar \sum_{q^{\perp}>0} \omega(\vec{q})\vec{v}_{\vec{q}} n^{+}_{\vec{q}}(y)$$

Thermal conductivity (from Fourier's Law)

$$\kappa^{+/-}(y) \; = \; |\vec{Q}^{+/-}(y)|/|\nabla T|$$

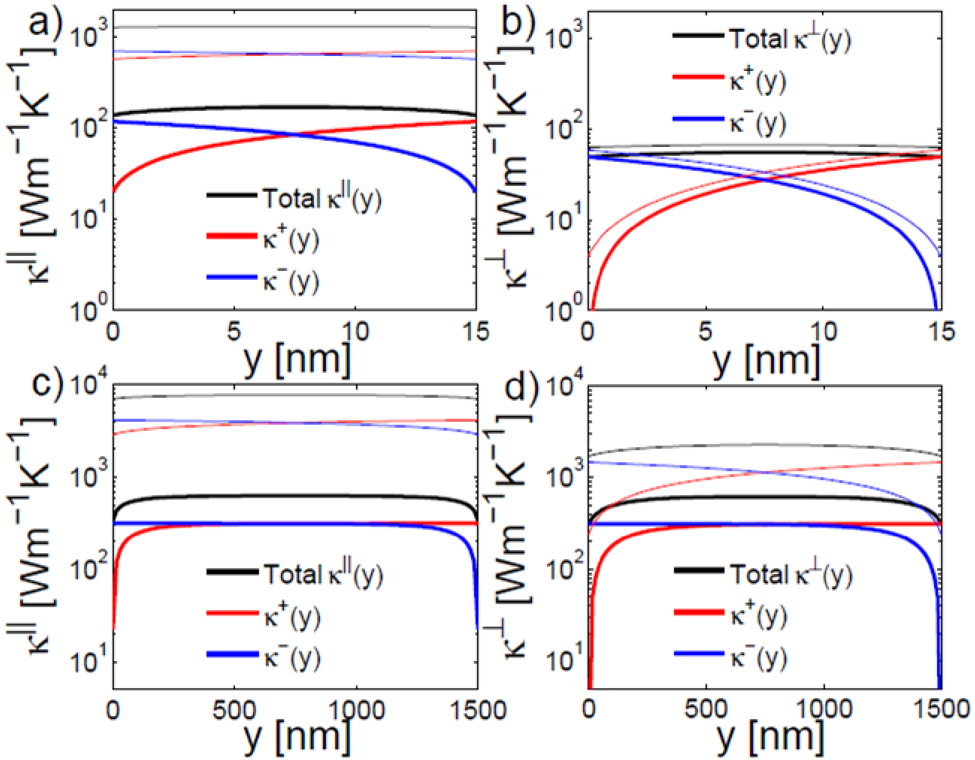

Wide versus narrow – in narrow ribbons (a,b) transport is dominated by edges and LER scattering, in wide ones (c,d) thermal transport dominated by internal (phonon-phonon)

Thermal transport in GNRs is size dependent

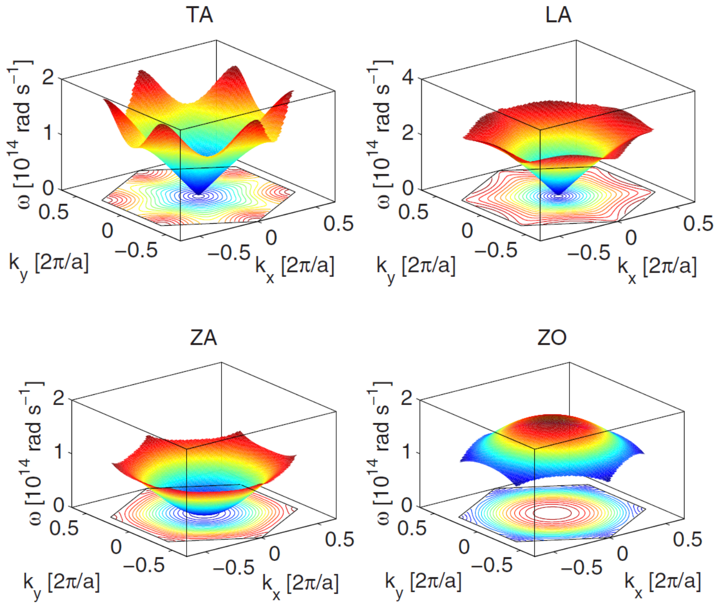

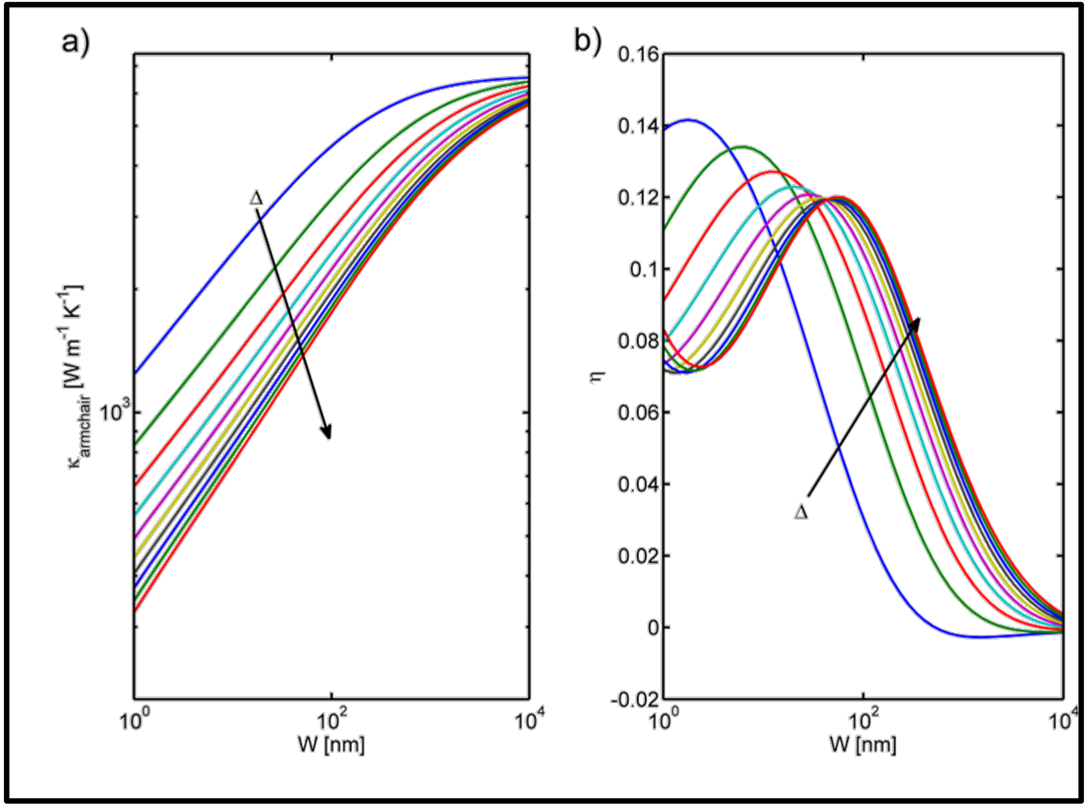

Z. Aksamija and I. Knezevic, Appl. Phys. Lett. v.98, 141919 (2011)

Thermal transport in narrow GNRs is anisotropic

- Angular depence of thermal conductivity reveals rich and complex behavior, especially in narrow and rough ribbons
- Zig-zag edge ribbons have up to 20% higher thermal conductivity than their armchair counterparts

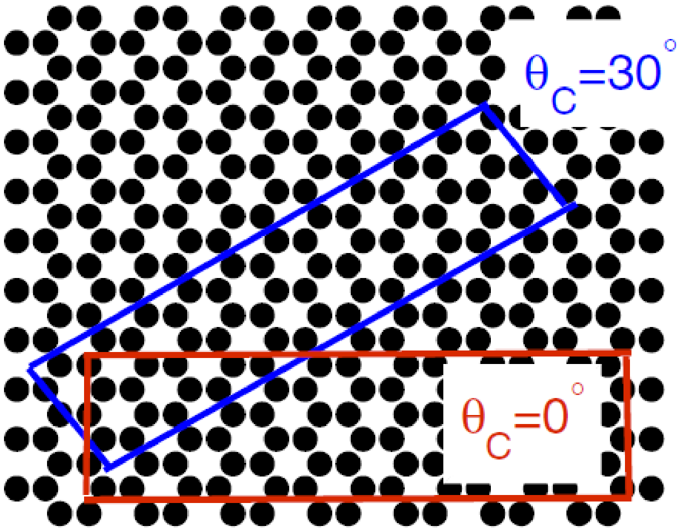

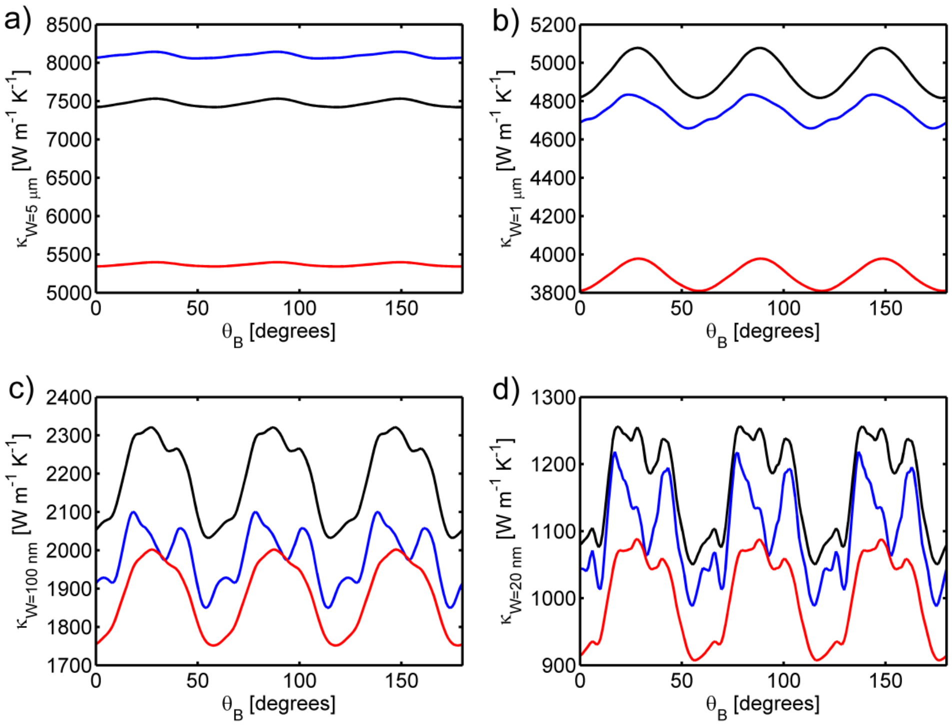

Z. Aksamija and I. Knezevic, Appl. Phys. Lett. v.98, 141919 (2011)

Thermal transport in supported graphene

- Substrate scattering due to van der Waals interaction
- Results agree closely with experimental data
  (Seol et al., Science 2010)
- Drastic reduction in narrow GNR samples
- Thermal transport in narrow GNRs is highly anisotropic

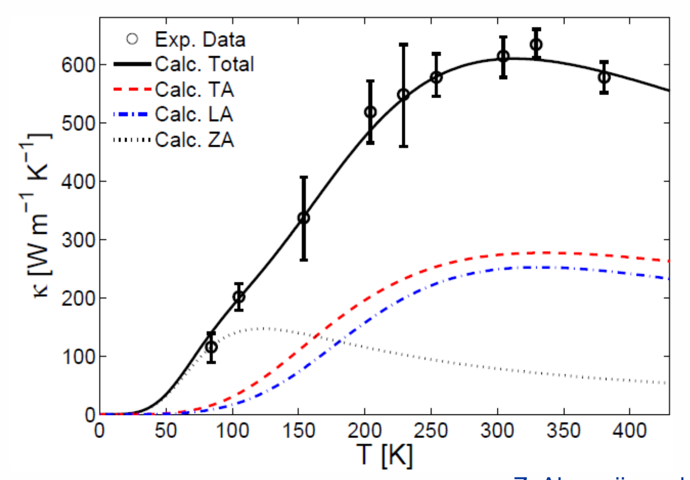

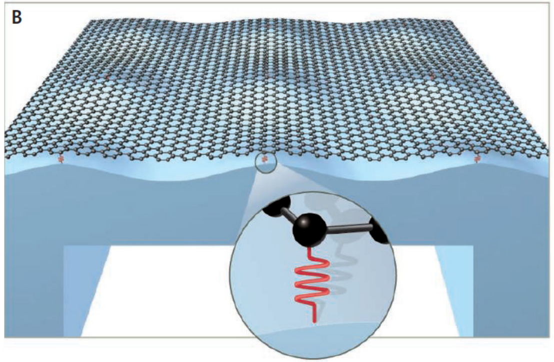

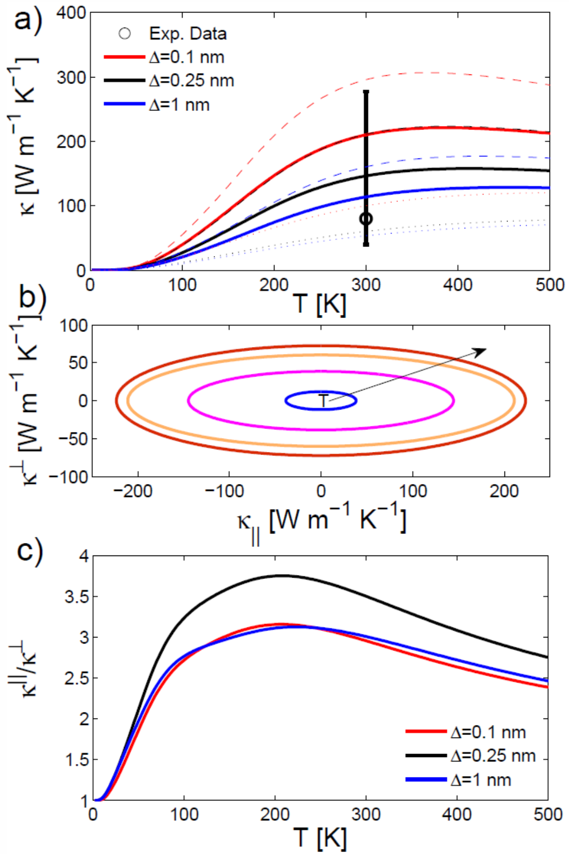

Z. Aksamija and I. Knezevic, Phys Rev. B,vol. 86, 165426 (2012).

Ballistic-to-diffusive transition in short GNRs

UMassAmherst

- Collaboration with Eric Pop's group (UIUC/Stanford)
- Transport in short GNRs is partially ballistic when length is comparable to twice the phonon mean-free-path (~100 nm)

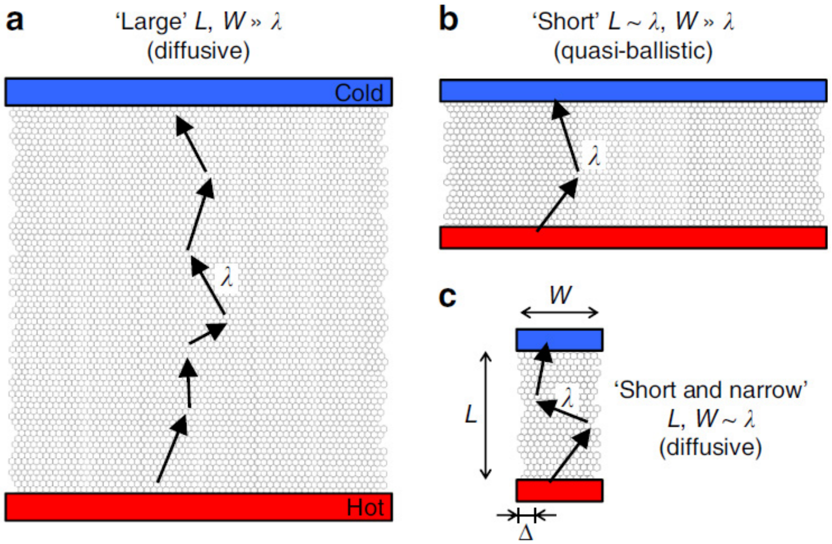

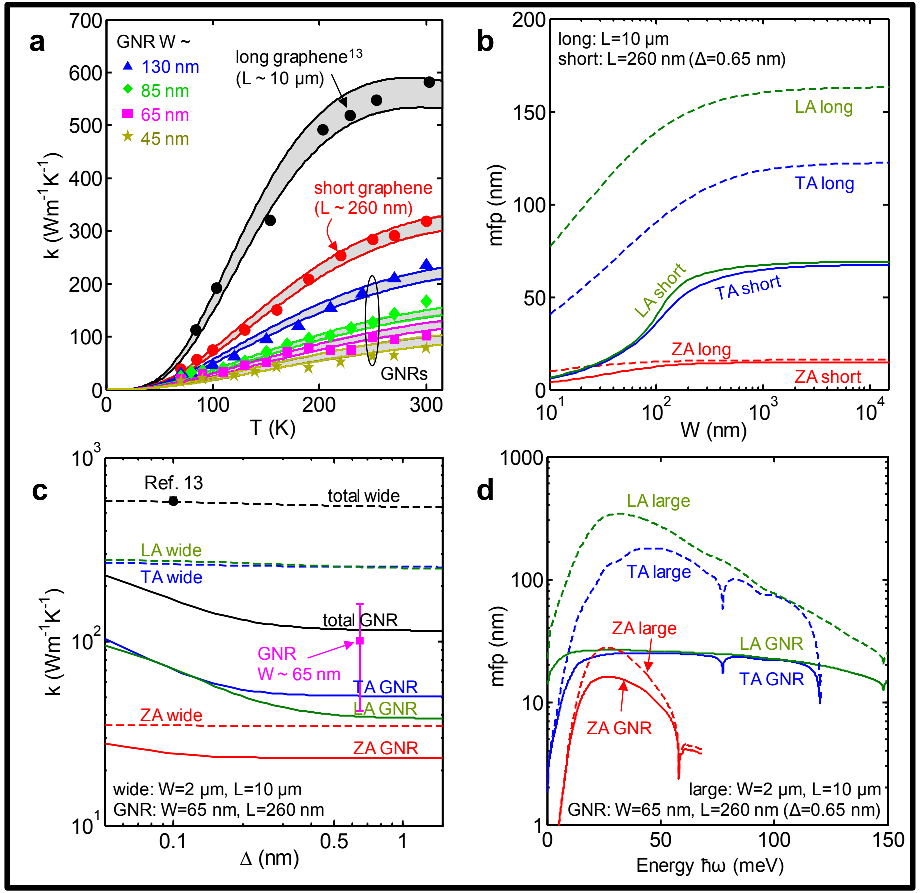

Bae, Li, Aksamija, et al., Nature Comm. 4, 1734 (2013)

UMassAmherst

Thermal transport in graphene GBs

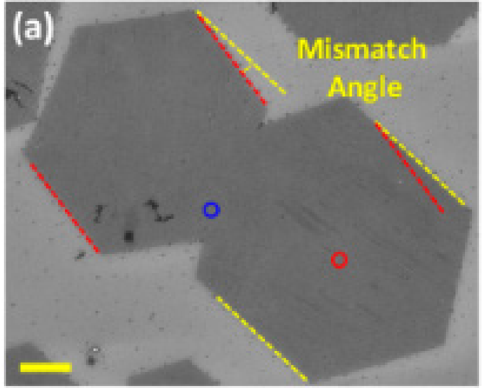

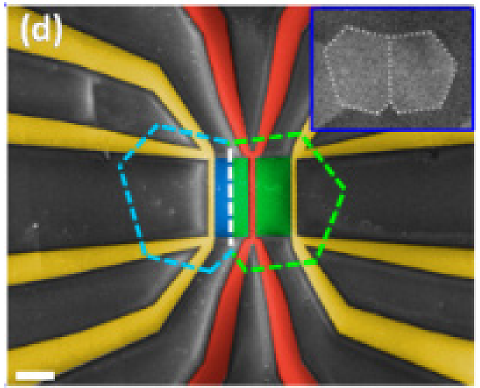

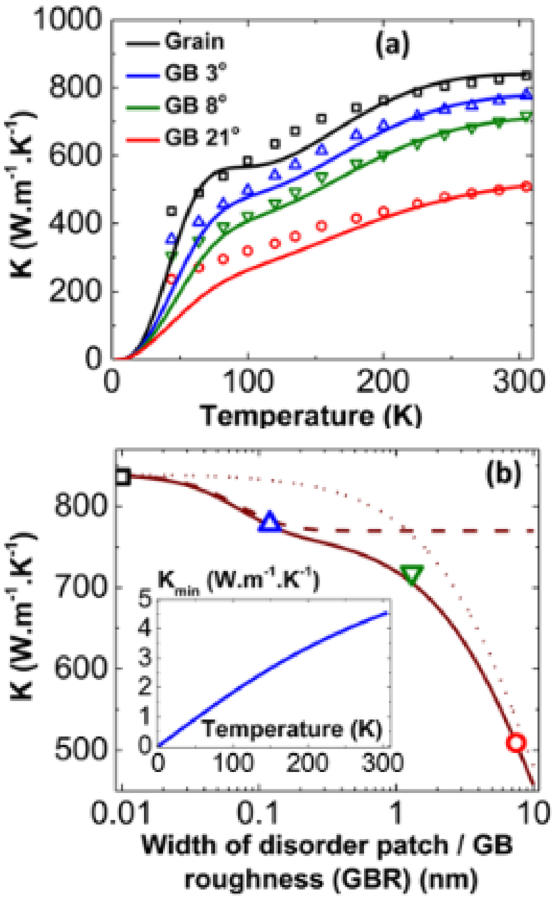

Yasaei et al., Nano Lett. 15, 4532, 2015

Grain boundaries deteriorate conductivity of a material, both thermal as well as electrical.

Thermal conductivity varies strongly with GB mismatch angle

Explained by phonon scattering from GB disorder

Thermal transport in CVD-grown graphene

UMassAmherst

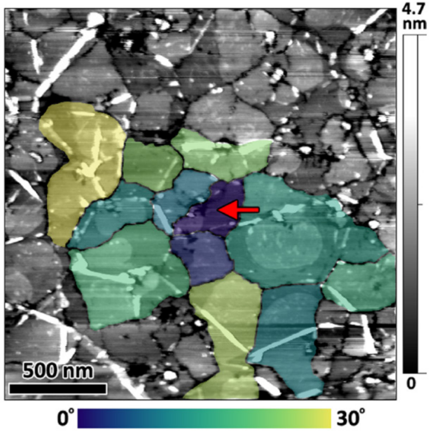

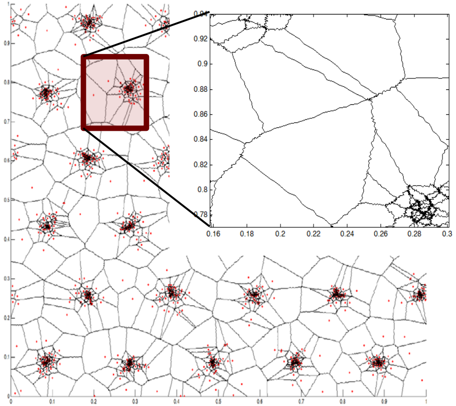

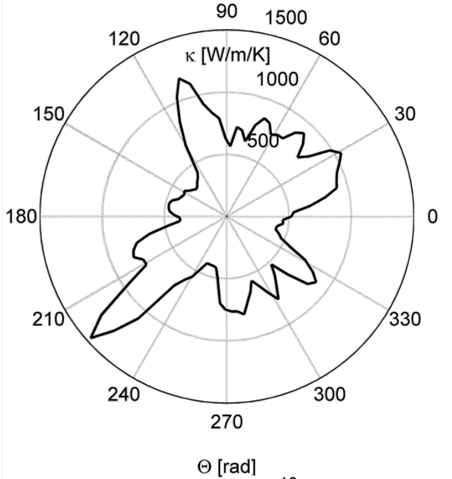

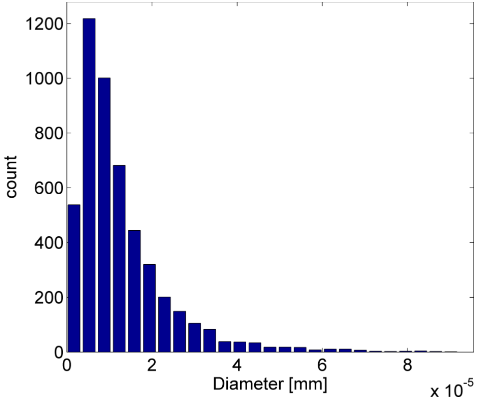

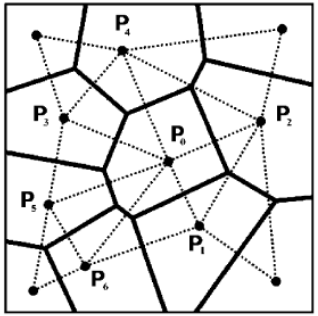

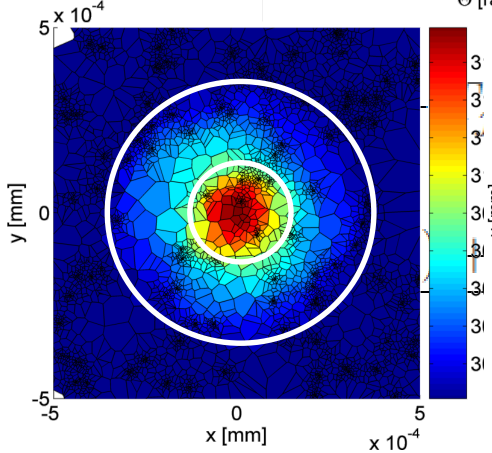

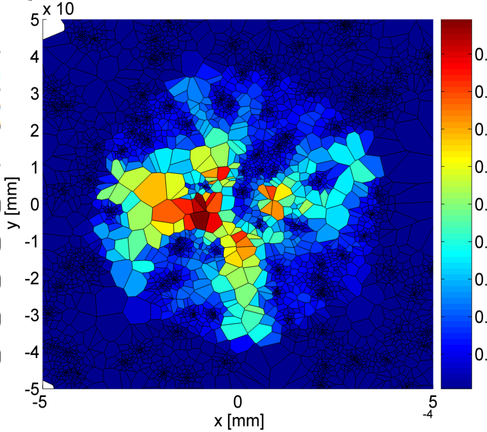

Z. Aksamija and I. Knezevic, PRB 90, 035419 (2014)

Length divergence in suspended ribbons

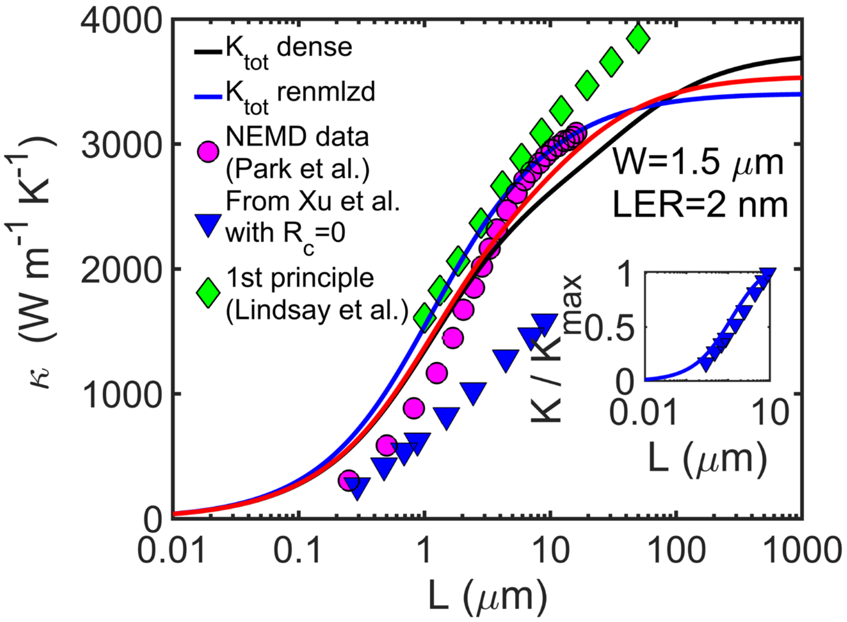

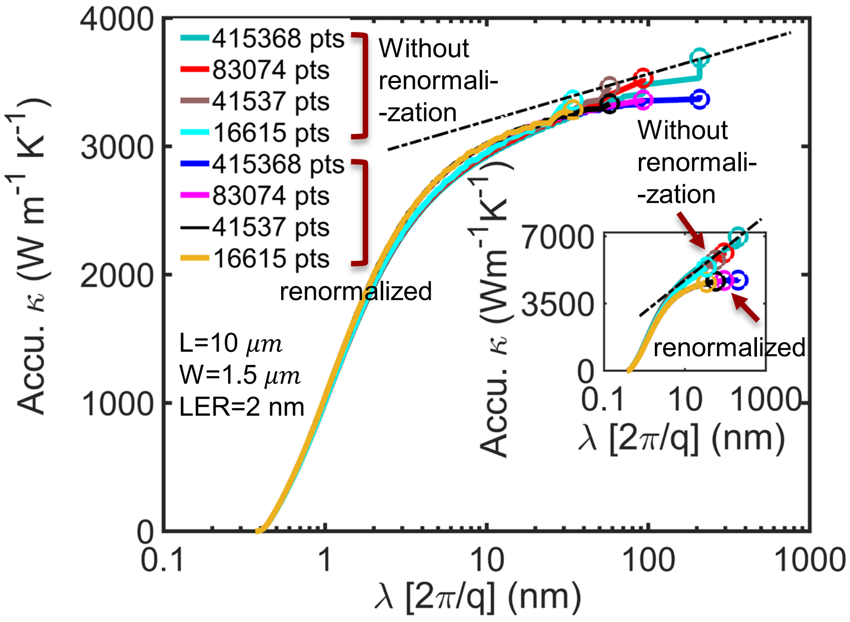

Xu et al., Nat. Commun. 5, 3720 (2014).
Lindsay et al., Phys. Rev. B 89, 155426 (2014).
Park et al, J. Appl. Phys. 114, 053506 (2013).
A.K. Majee and Z. Aksamija Phys. Rev. B 93, 235423,2016.

Effect of width and edge roughness

UMassAmherst

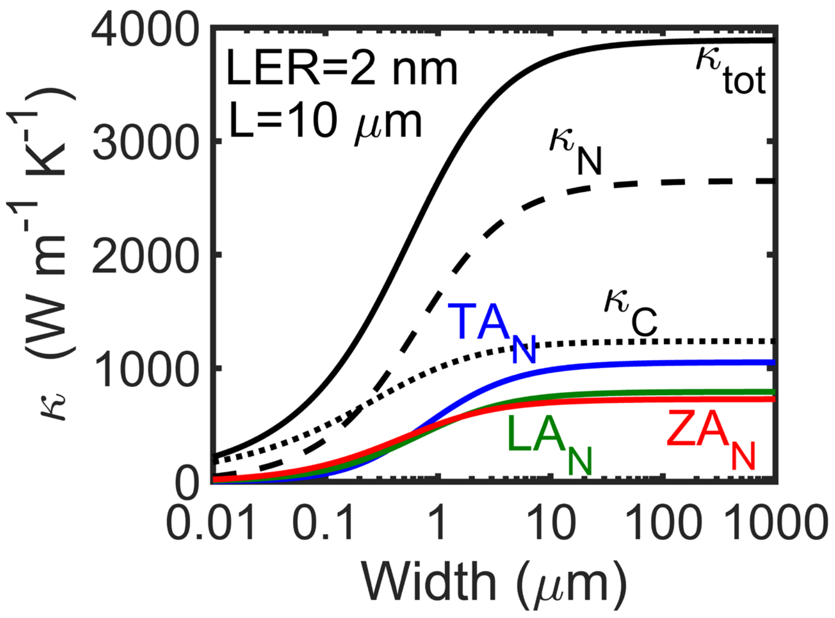

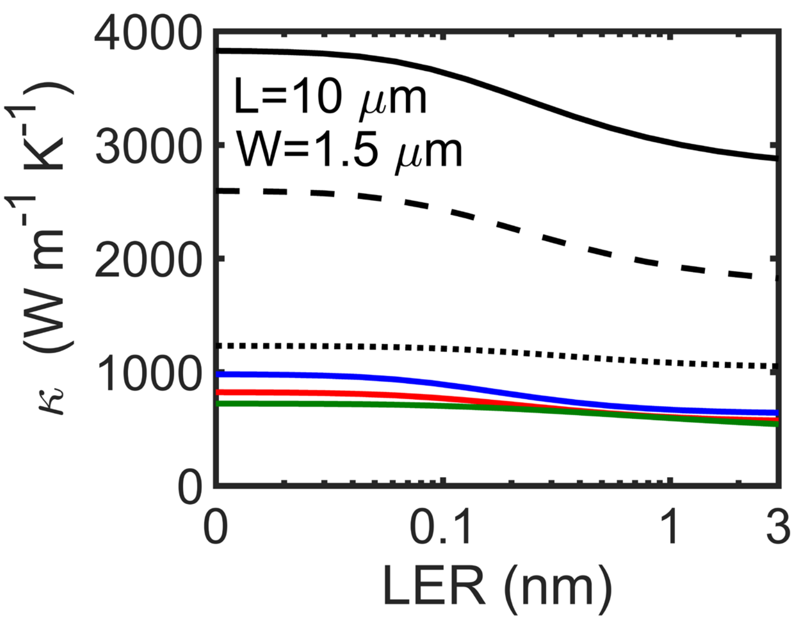

Strong width dependence of thermal conductivity in graphene ribbons arising from the dependence of normal contribution and the interplay between LER and normal scattering

A.K. Majee and Z. Aksamija Phys. Rev. B 93, 235423,2016.

Methodology (contd.)

Taking Fourier transform of BTE

$$j\Omega n_q + v_q \frac{\partial n_q^0}{\partial T} \cdot \nabla T = -\frac{\Phi_q}{\tau_C} - \frac{1}{\tau_N}\frac{k_B T^2}{\hbar\omega_q}\frac{\partial n_q^0}{\partial T}\vec{\Lambda}.\vec{q}$$

Where $\Phi_q = n_q - n_q^0$

Rearranging the terms to solve for Φ_q

$$\Phi_q = -\frac{\tau_C}{1 + j\Omega\tau_C}(v_q \cdot \nabla T)\frac{\partial n_q^0}{\partial T} - \frac{\tau_C/\tau_N}{1 + j\Omega\tau_C}\frac{k_B T^2}{\hbar\omega_q}\frac{\partial n_q^0}{\partial T}\vec{\Lambda}.\vec{q}$$

Normal scattering conserves momentum [5]

$$\sum_q q(n_q - n_q^*) = 0 = \sum_q q(\Phi_q + n_q^0 - n_q^*)$$

Substituting for $n_q^0 - n_q^* = n_q^0(n_q^0 + 1)\vec{\Lambda}.\vec{q}$, we get

$$\Lambda = \frac{\sum_q q\left(\frac{\tau_C}{1 + j\Omega\tau_C}(v_q \cdot \nabla T)\frac{\partial n_q^0}{\partial T}\right)}{\sum_q q^2 \frac{\partial n_q^0}{\partial T}\frac{k_B T^2}{\hbar\omega_q}\left(1 - \frac{\tau_C/\tau_N}{1 + j\Omega\tau_C}\right)}$$

5. P.B. Allen, Phys. Rev. B 88, 144302,2013.

Methodology (contd.)

Heat current in Fourier space

$$\vec{J}(\Omega) = \sum_q \hbar\omega_q v_q \Phi_q(\Omega) = -\kappa(\Omega)\nabla T(\Omega)$$

We get two components of thermal conductivity

$$\kappa_{tot}(\Omega) = \kappa_{\mathrm{C}}(\Omega) + \kappa_{\mathrm{N}}(\Omega)$$

$$= \kappa_{\mathrm{C}}(\Omega) + \sum_b \frac{\lambda_{1,b}(\Omega)\lambda_{2,b}(\Omega)}{\lambda_{3,b}(\Omega)}$$

Thermal conductivity due to single-mode relaxation approximation

$$\kappa_C(\Omega) = \frac{1}{A\delta}\sum_{q,b} \hbar\omega_{q,b}\, v_\parallel^2(q,b) \frac{\tau_C(q,b)}{1 + j\Omega\tau_C(q,b)} \frac{\partial n_{q,b}}{\partial T}$$

Correction to thermal conductivity due to collective excitation of phonons due to anharmonic phonon-phonon processes

$$\lambda_{1,b}(\Omega) = \frac{1}{A\delta}\sum_{q,b} q_\parallel\, v_\parallel(q,b) \frac{\tau_C(q,b)}{1 + j\Omega\tau_C(q,b)} \frac{\partial n_{q,b}}{\partial T}$$

$$\lambda_{2,b}(\Omega) = \frac{1}{A\delta}\sum_{q,b} q_\parallel\, v_\parallel(q,b) \frac{\tau_C(q,b)/\tau_N(q,b)}{1 + j\Omega\tau_C(q,b)} \frac{\partial n_{q,b}}{\partial T}$$

$$\lambda_{3,b}(\Omega) = \frac{1}{A\delta}\sum_{q,b} \frac{q_\parallel^2}{\hbar\omega_{q,b}} \left[1 - \frac{\tau_C(q,b)/\tau_N(q,b)}{1 + j\Omega\tau_C(q,b)}\right] \frac{\partial n_{q,b}}{\partial T}$$

Frequency-dependent thermal conductivity

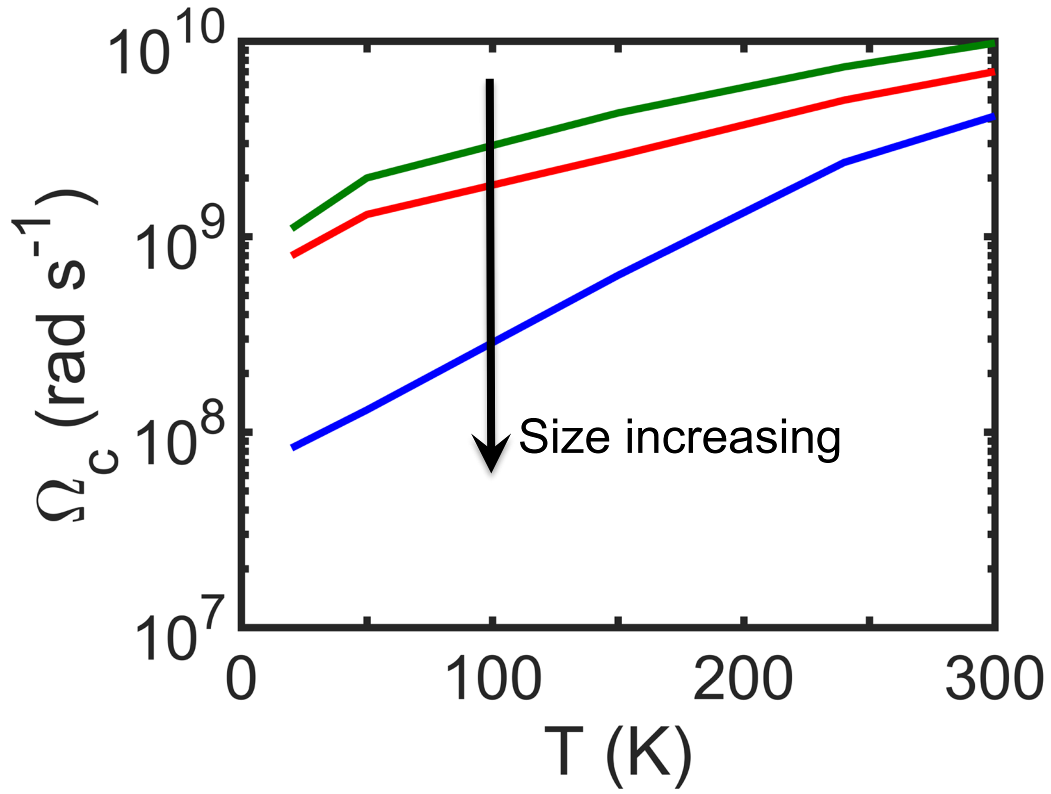

A. K. Majee and Z. Aksamija, Phys. Rev. B **98**, 024303 (2018)

Analogous to frequency-dependence of electrical conductivity

$$\kappa(\Omega) = \frac{\kappa_0}{1 + j\Omega\tau_C}$$

Resembles low pass thermal filter with cut-off frequency defined as the frequency where $\kappa(\Omega_C) = 0.707\kappa_0$

Curves	Length (μm)	Width (μm)
Blue line	100	100
Red line	10	10
Green line	10	1.5

Low-pass filter like response

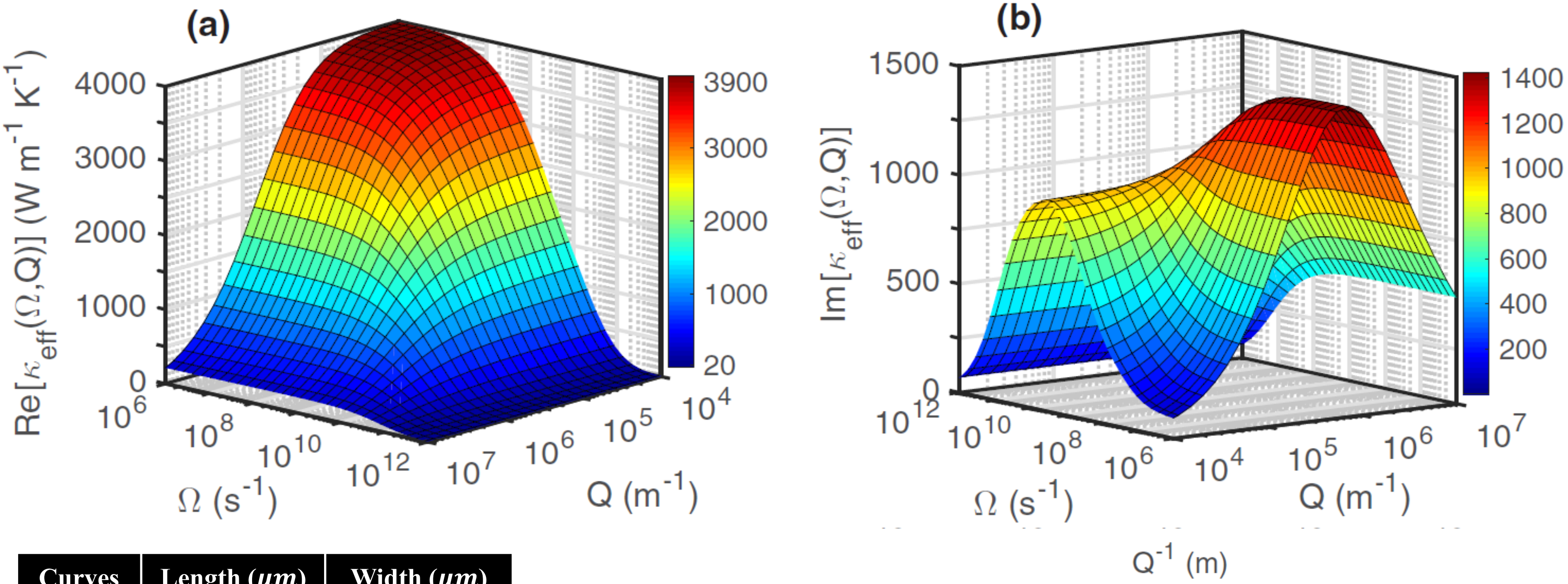

Curves	Length (μm)	Width (μm)
	100	100
	10	10
	10	1.5

$$mean\ free\ path = \frac{\sum_{q,b} \hbar\omega_{q,b}\, v_{\parallel}^2(q,b) \frac{\tau_C(q,b)}{1 + j\Omega\tau_C(q,b)} \frac{\partial n_{q,b}}{\partial T}}{\sum_{q,b} \hbar\omega_{q,b}\, v_{\parallel}(q,b)\, \frac{\partial n_{q,b}}{\partial T}}$$

Resistive and normal contribution

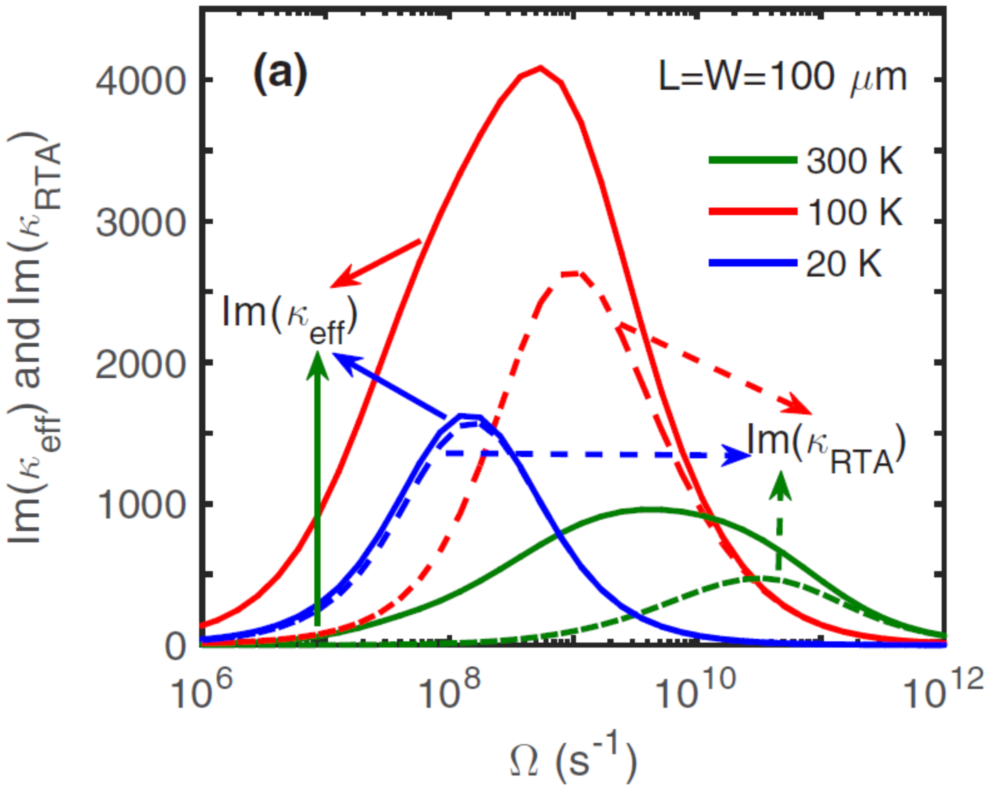

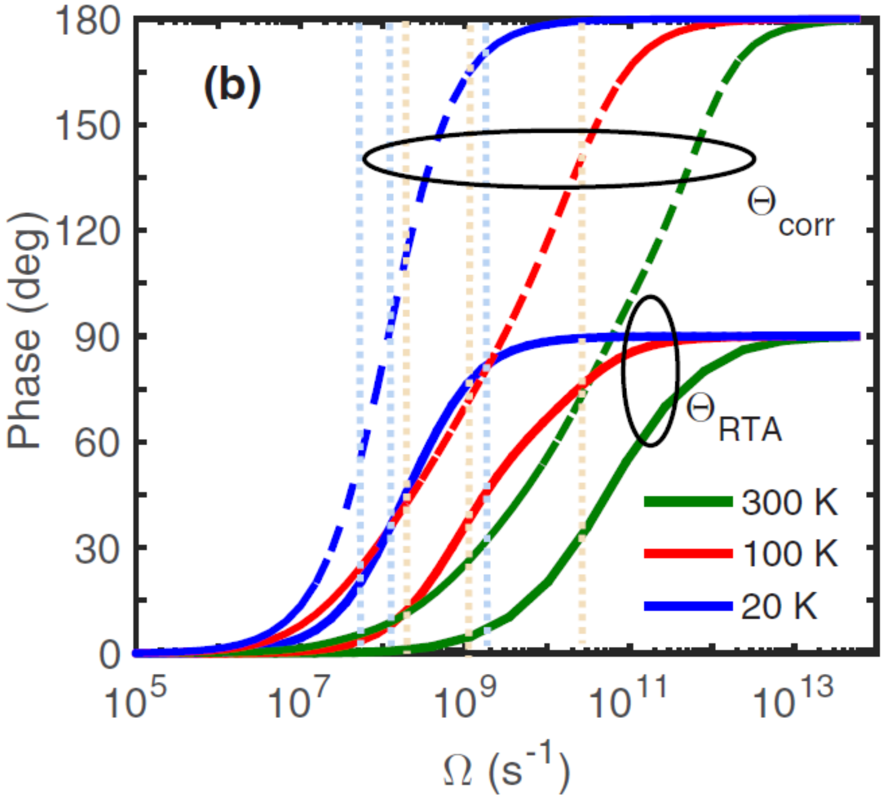

Conclusion (pt. 1)

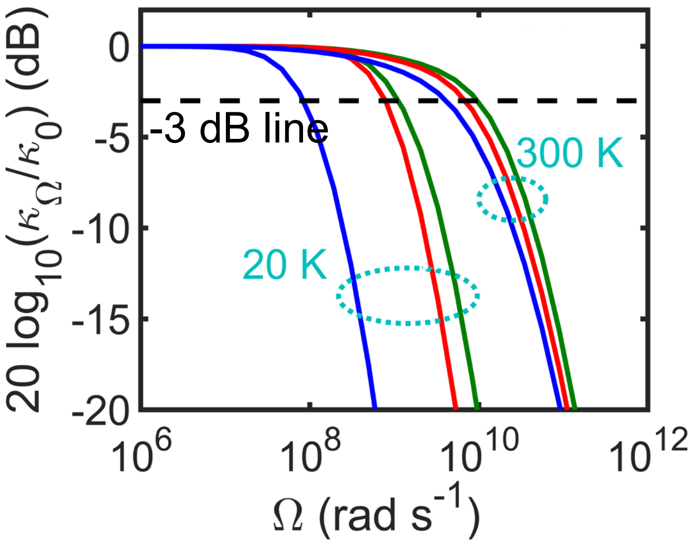

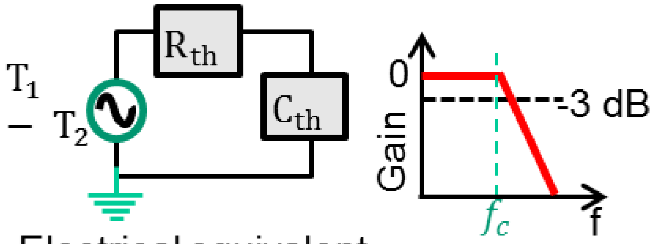

Electrical equivalent of thermal circuit

- Dynamical response of thermal conductivity resembles like a low-pass thermal filter characteristics.
- The equivalent circuit has both resistance and capacitance---the latter arising from energy stored by phonons between their scattering events
- The cut-off frequency is found to be proportional to the scattering rates
- Can be tuned over a wide range—100 MHz to 10 GHz —by varying ribbon size and temperature.
- This technique could be used to probe phonon mean-free-path spectrum

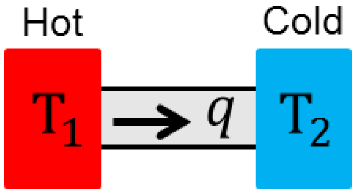

Growing interest in lateral 2D heterostructures

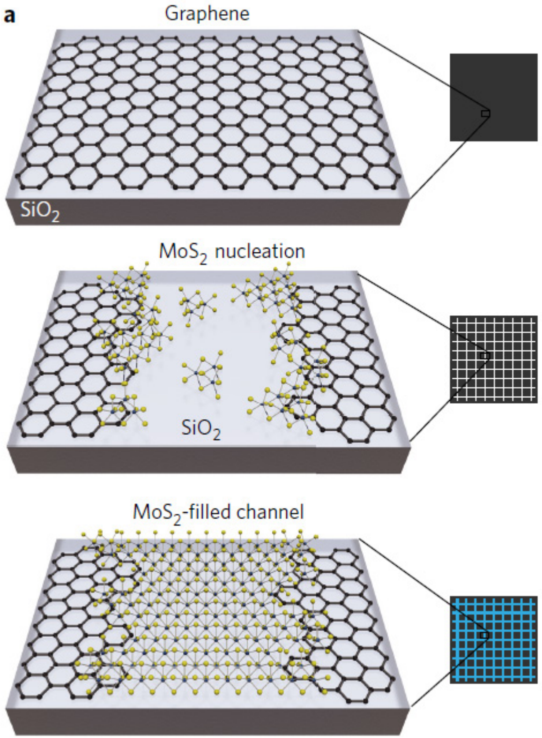

Zhao et al., Nat. Nano, 11, 954-959 (2016)

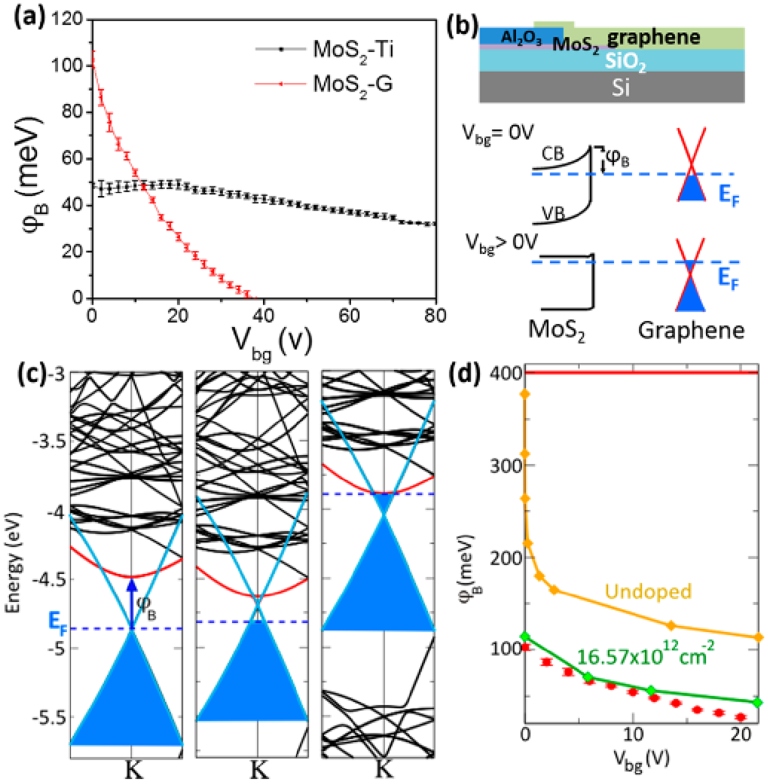

Yu et al., Nano Lett., 14, 3055-3063 (2014)

Graphene-MoS_2 heterojunction FET

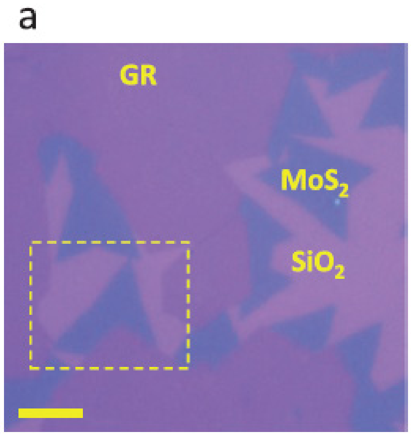

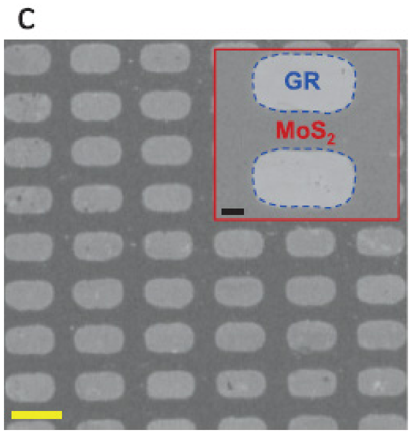

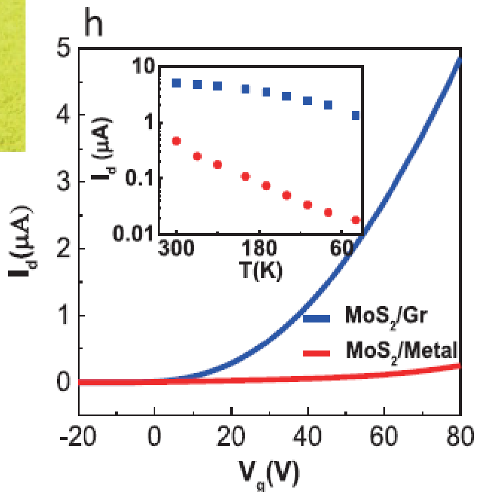

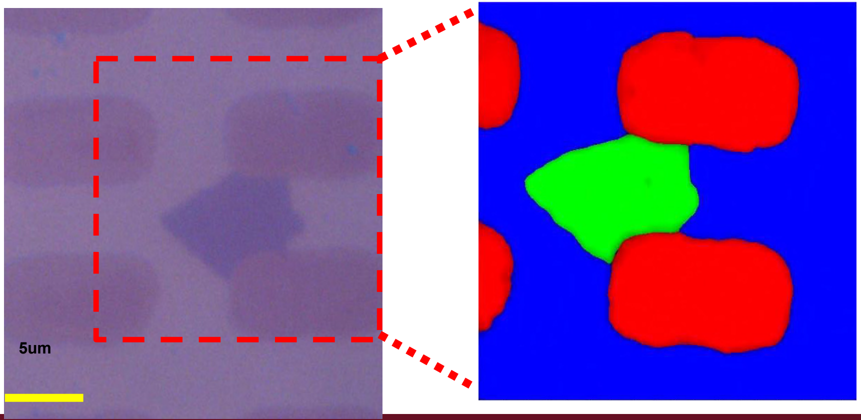

SEM (left) and Raman map (right) of individual MoS_2 flake grown between graphene electrodes

Behranginia et al. Small 1604301 (2017)

Band structure calculation and alignment at the interface

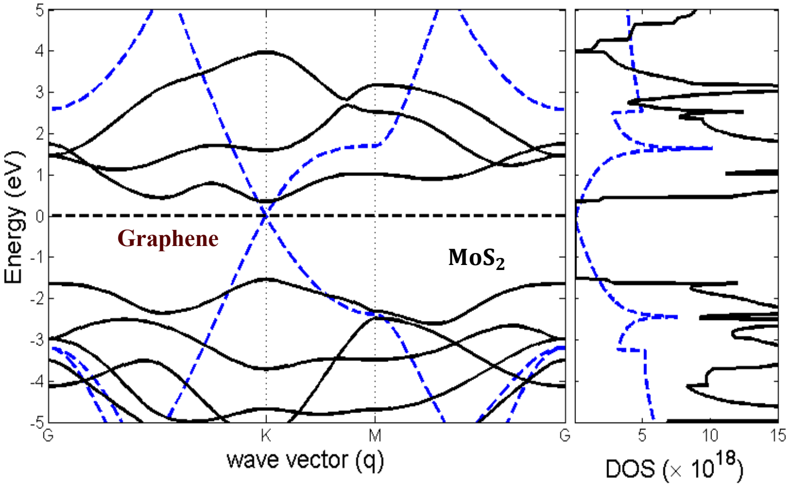

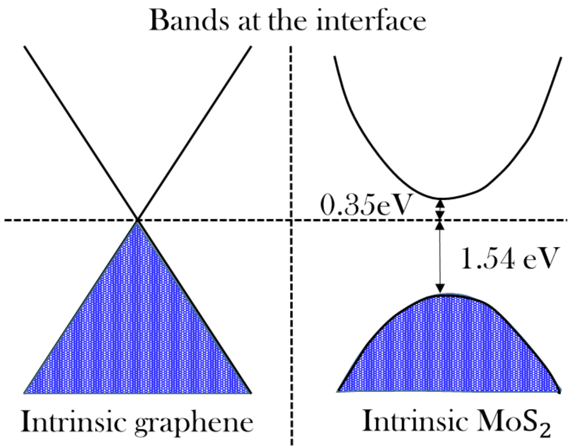

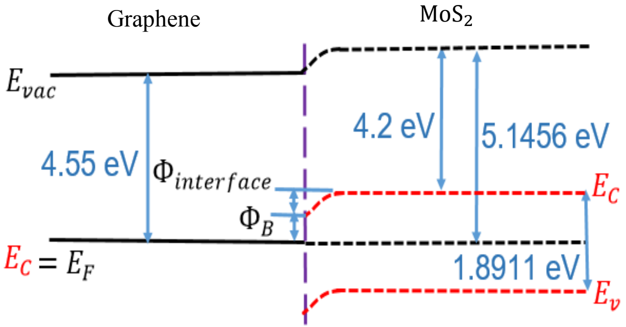

V_g=0 V, intrinsic

$$\phi = \chi + (E_c - E_F)$$

$$\phi_B(V_g) = \phi_{grap}(V_g) - \chi_{MoS2}$$

$$\phi_{interface}(V_g) = \phi_{MoS2}(V_g) - \chi_{MoS2} - \phi_B(V_g)$$

Calculation of grain boundary resistance

Transport distribution function

$$\Xi(E) = \sum_b v_b(E)\Gamma_b(E)D_b(E)$$
$$= \sum_b \frac{1}{4\pi^2}\int v_b(k)\,\tau_b(k)\delta\big(E - E_b(\mathbf{k})\big)d\mathbf{k}$$

Using Landauer formalism, we compute interface conductance

$$R_{int}^{-1} = G_{int} = \frac{e^2}{2}\int_{E_C}^{E_{max}} \Xi(E)\left(-\frac{\partial f(E-E_F,T)}{dE}\right)dE$$

Fermi window

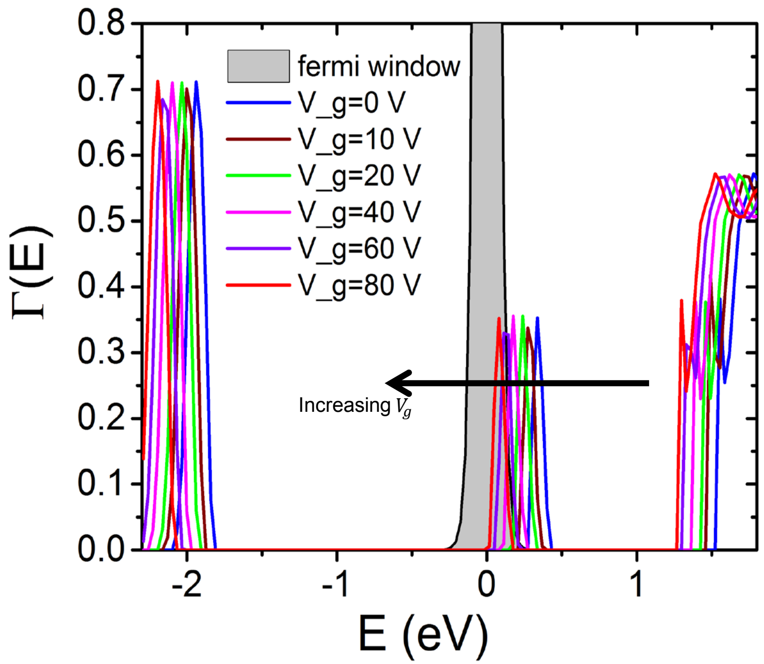

- Transport occurs inside the Fermi window
- Transmission depends on gate voltage due to band alignment

Nomenclature of the type of interfaces

In homojunctions (same material on either side of the interface):

When $\theta_L = \theta_R$ ⟶ **TWIN GBs**

$\theta_L \neq \theta_R$ ⟶ **TILT GBs**

$\theta_L = 0$, $\theta_R = \theta_M$ ⟶ **Most disordered TILT GBs**

In heterojunctions:
(Different materials on either side of the interface):

When $\theta_L = \theta_R$ ⟶ **Class-I interface**

$\theta_L \neq \theta_R$ ⟶ **Class-II interface**

$\theta_L = 0$, $\theta_R = \theta_M$ ⟶ **Most disordered Class-II interface**

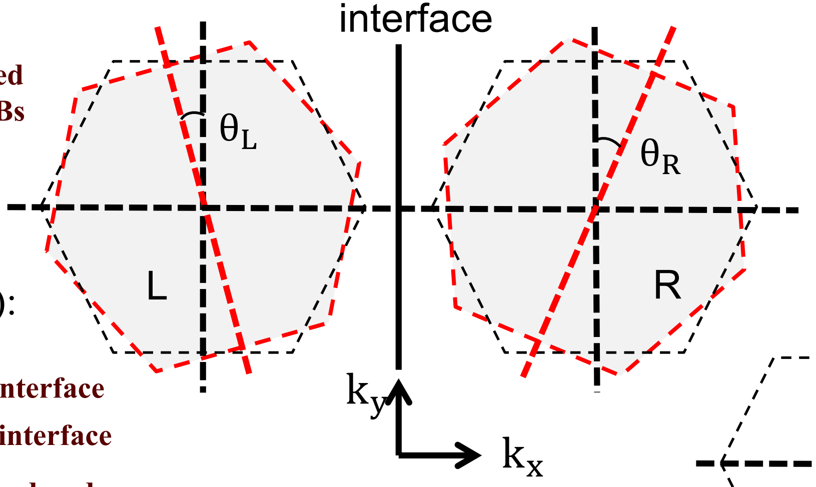

$$\theta_M = \theta_L + \theta_R$$
$$\theta_L = \theta_R$$

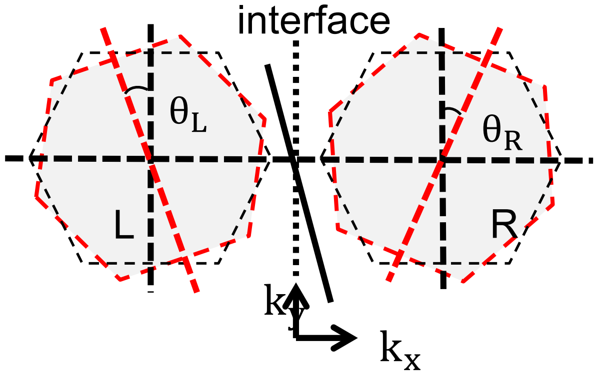

$\theta_M = 8°, \theta_L = 3°, \theta_R = 5°, \theta_B = 1°$
Tilt GBs

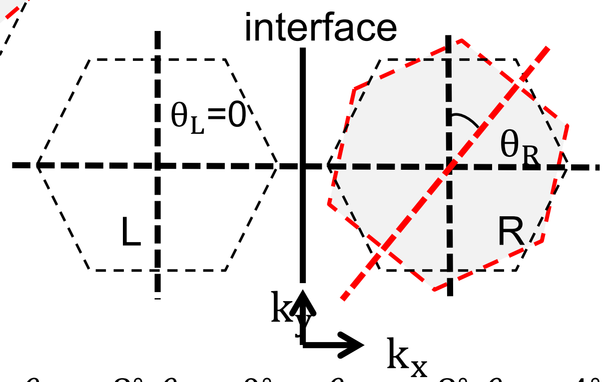

$\theta_M = 8°, \theta_L = 0°, \quad \theta_R = 8°, \theta_B = 4°$
Most disordered Tilt GBs

Graphene-Graphene GB resistance

Twin GBs ($\theta_L = \theta_R$)

No transmission gap.

Even large mismatch angles don't lead to very high GB resistance.

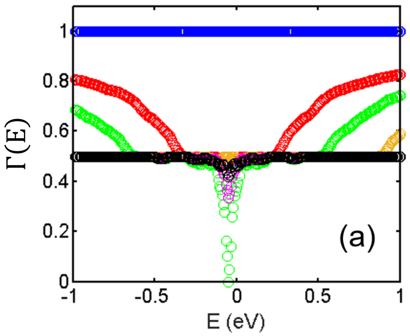

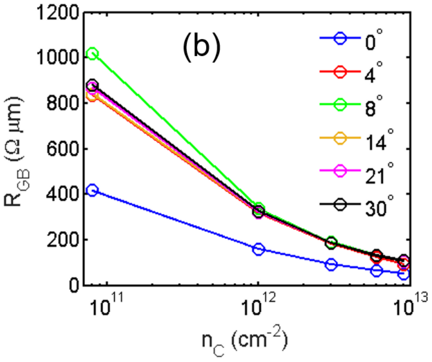

$n_C = 1 \times 10^{12}\ cm^{-2}$

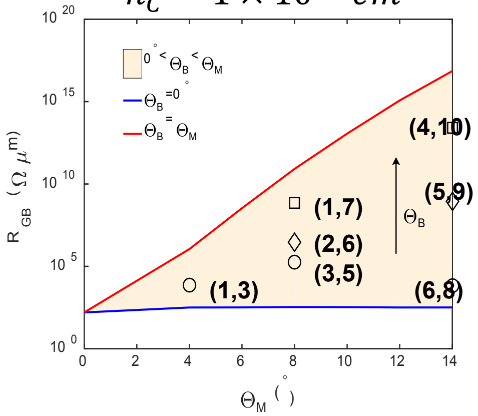

$n_C = 9 \times 10^{12}\ cm^{-2}$

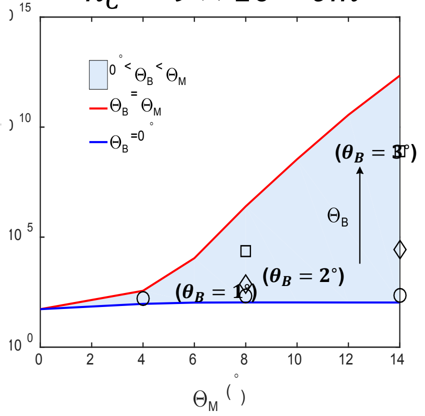

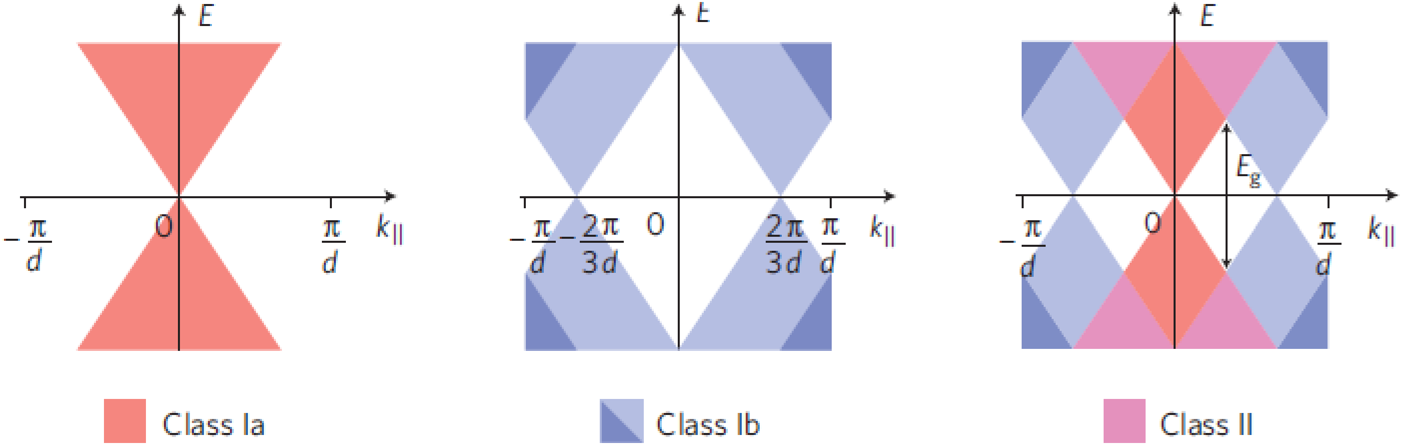

Oleg V. Yazyev and Steve G. Louie (2010) Electronic transport in polycrystalline graphene.

MoS_2-MoS_2 GB resistance

Twin GBs ($\theta_L = \theta_R$)

No transmission gap, just band gap

Even large mismatch angles don't lead to very high GB resistance.

Tilt GBs ($\theta_L = 0°, \theta_R = \theta_M$)

Transmission gap opens up for large mismatch angles.

Doesn't exhibit a strong mismatch angle dependence as compared to graphene tilt GBs.

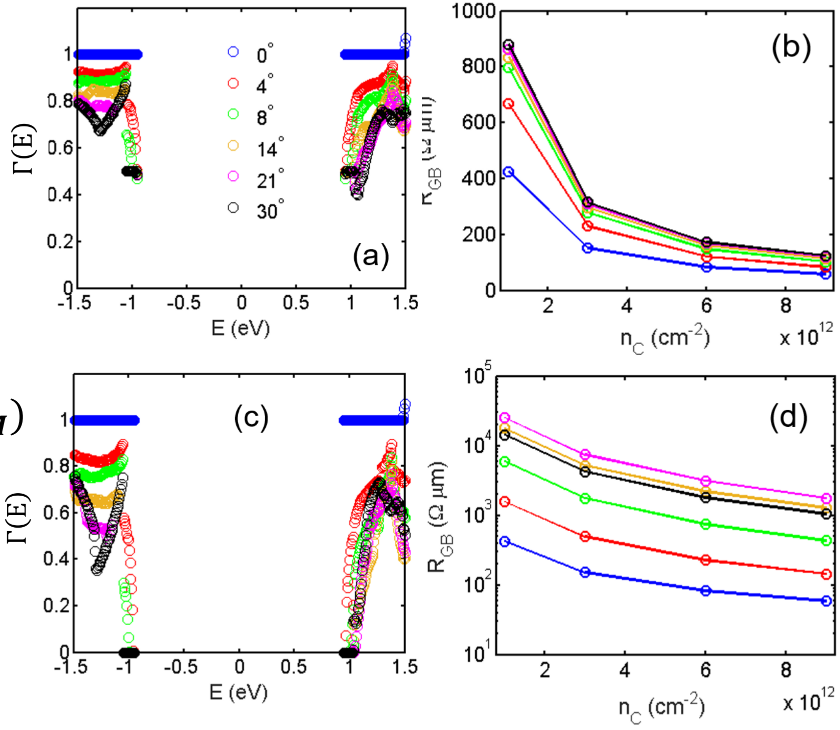

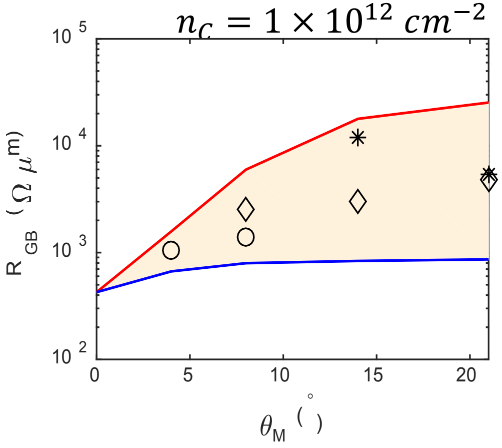

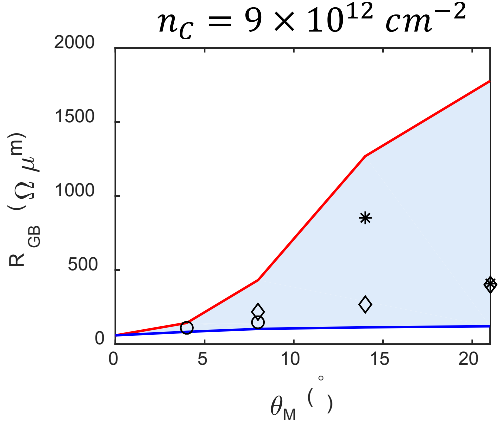

Graphene-MoS_2 interface resistance

Class I interface
$(\theta_L = \theta_R)$

No transmission gap.

Shows negligible angle dependence.

Exhibits strong dependence on carrier density.

Class II interface
$(\theta_L = 0°, \theta_R = \theta_M)$

Transmission gap opens up with increasing mismatch angles.

Exhibit a very strong dependence on both mismatch angle and carrier density.

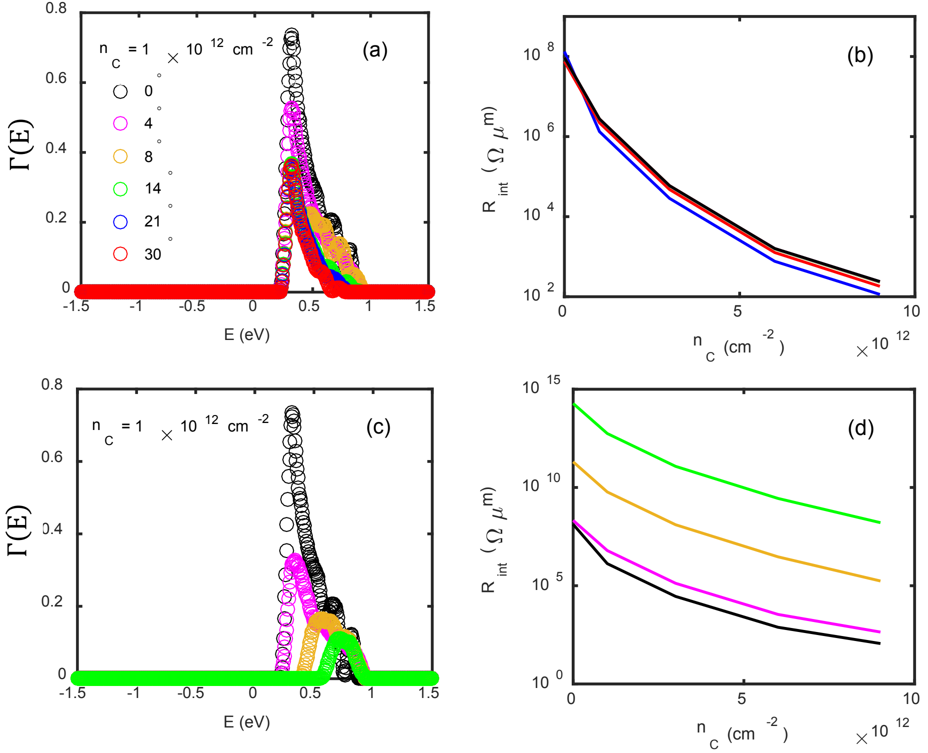

Comparison of interface/GB resistance

- Graphene/Graphene asymmetric GBs are highly resistive
- MoS_2/MoS_2 are not!
- Reason: graphene Dirac cones are steep and underlap when rotated
- MoS_2 bands are shallow (large effective mass) so they overlap more

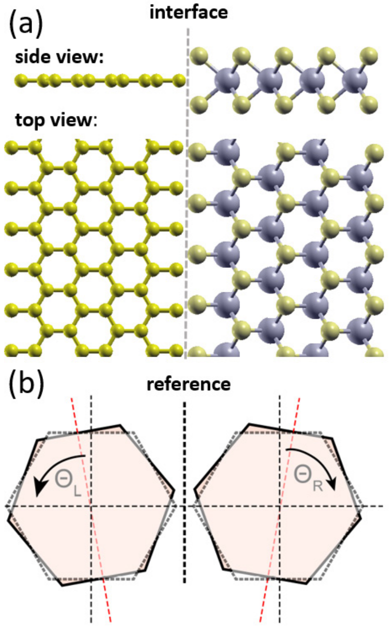

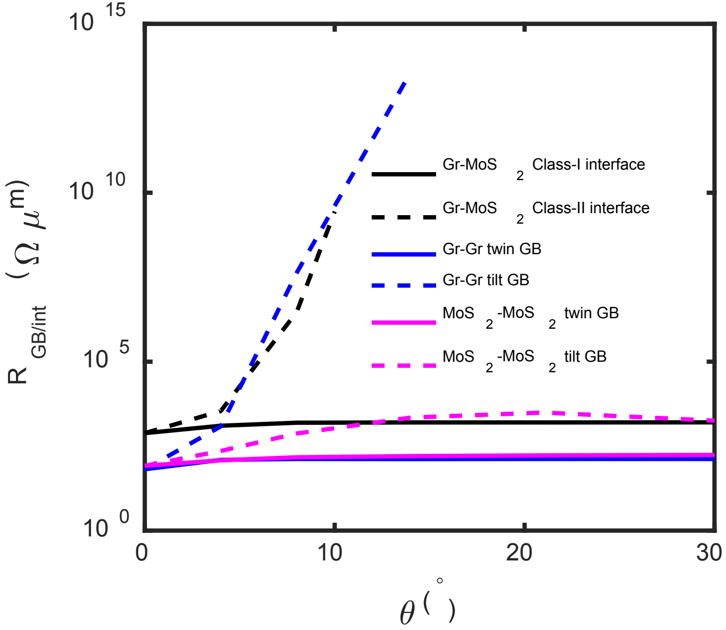

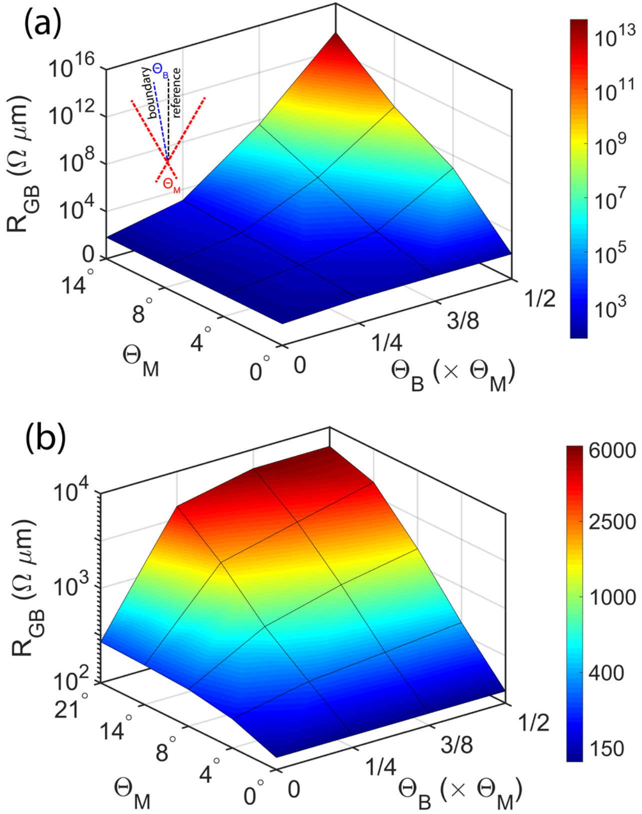

Comparison of GB resistivity with literature

UMassAmherst

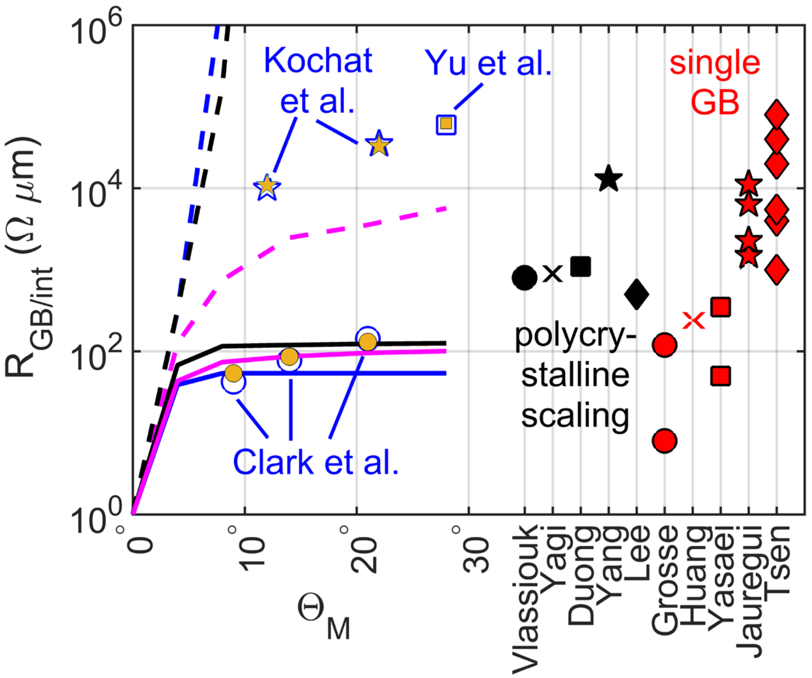

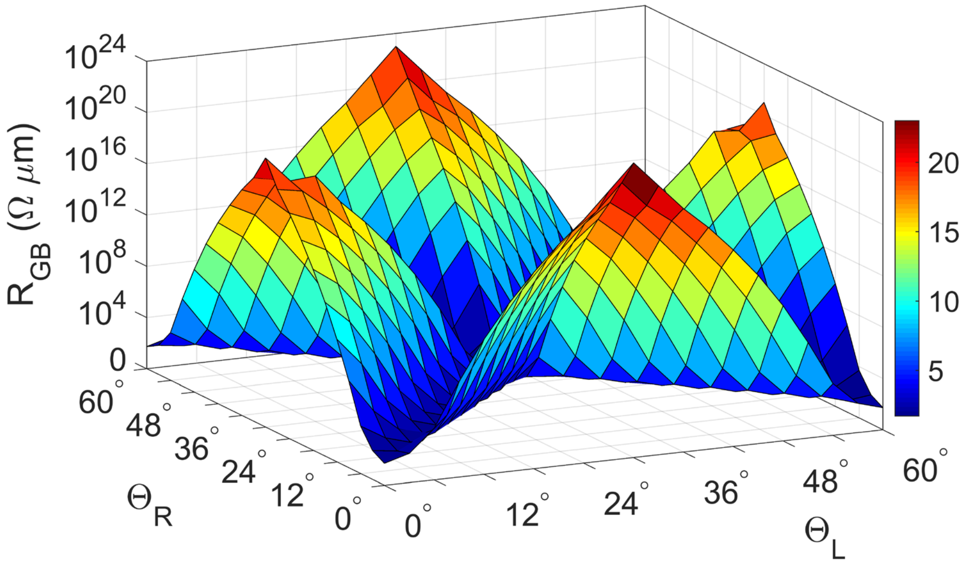

Majee, Foss, and Aksamija, Sci. Rep. 7, 16597, 2017

Majee, Kommini, and Aksamija, Ann. Phys.(Berlin), 531, 1800510 (2019)

Motivation, pt. 2

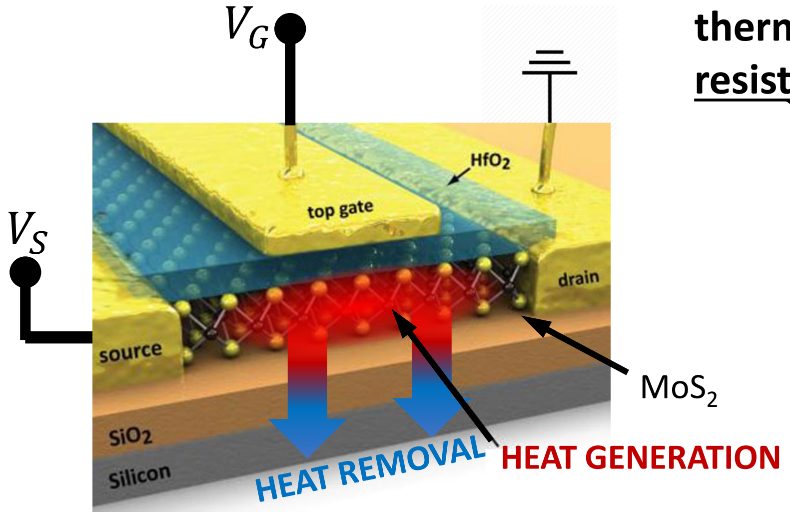

Overall thermal <u>resistance</u>

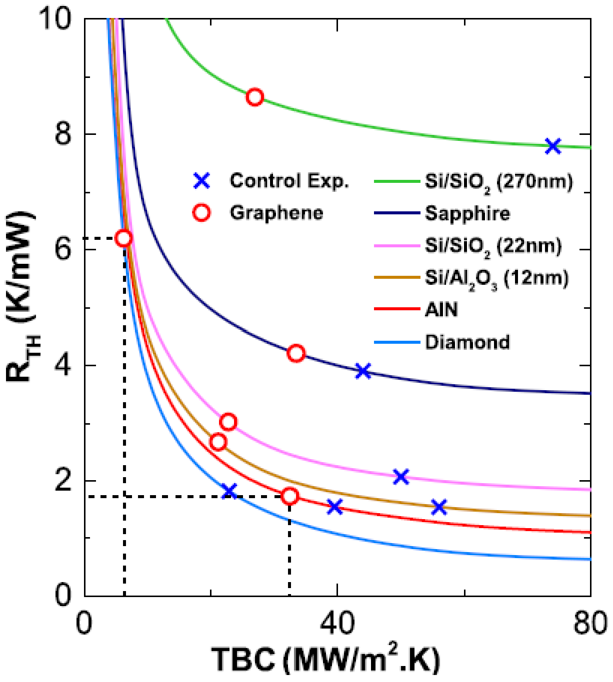

- Most heat generated in a 2D material based device dissipates into the supporting substrate.
- Hence, the thermal (2D/3D) interface formed strongly dictates the capabilities of thermal management in 2D devices.

What is the best substrate for 2D/3D TBC?

Can we map constituent material properties to the TBC and identify materials for improved TBC?

Nature Nano., vol. 6, p. 147–150, (2011).
2D Mater. **4** (2017) 035027

Methodology

- The substrate scattering rate based on Fermi's Golden Rule

$$\Gamma_{sub}(\omega) = \frac{\pi}{2}\frac{D_{sub}(\omega)}{m_{sub}m_{2D}}\frac{K_a^2}{\omega^2}$$

Then use a Landauer formalism to calculate the TBC G(T):

$$G(T) = \int C_{2D}(\omega, T)D_{2D}(\omega)\Gamma_{sub}(\omega)d\omega$$

- $G(T)$ (TBC) roughly follows K_a^2
- However, we want to decouple the influence of K_a and material properties on the TBC.
- At a constant K_a, $\Gamma_{sub} \propto \frac{1}{\omega^2}$ ➔ low-energy, long-wavelength phonons contribute most to TBC.
- 42 interfaces studied (6 2D layers and 7 substrates).

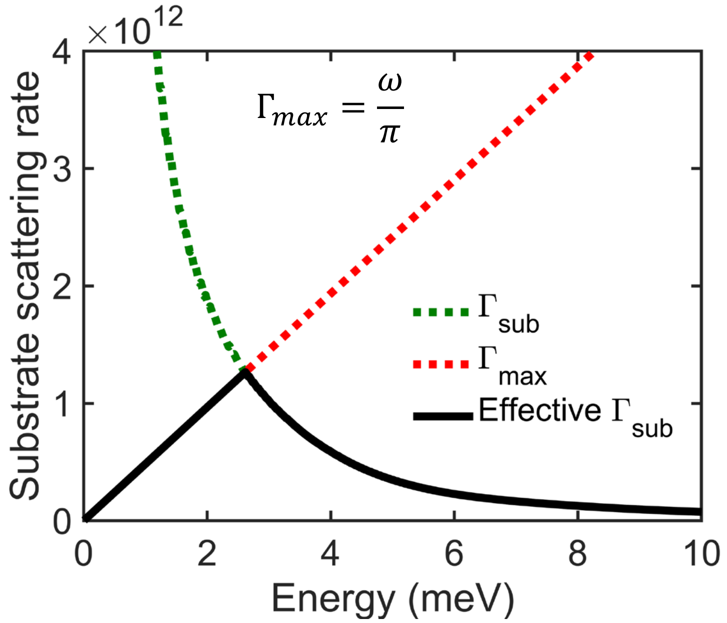

$E = \hbar\omega$

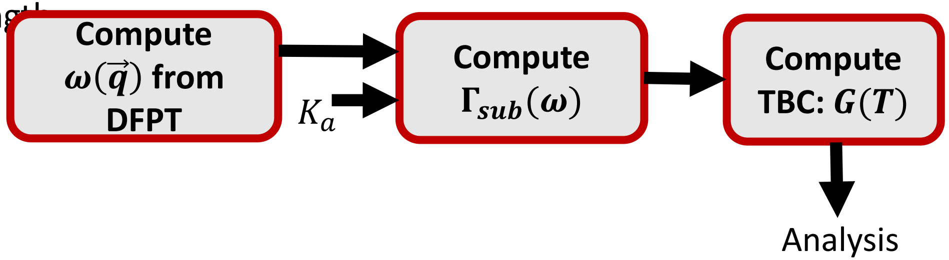

Nanotechnology 28 (2017) 135402
Adv. Mater. Interfaces (2017), 4, 1700334

2D-layer phonon dispersion on substrate

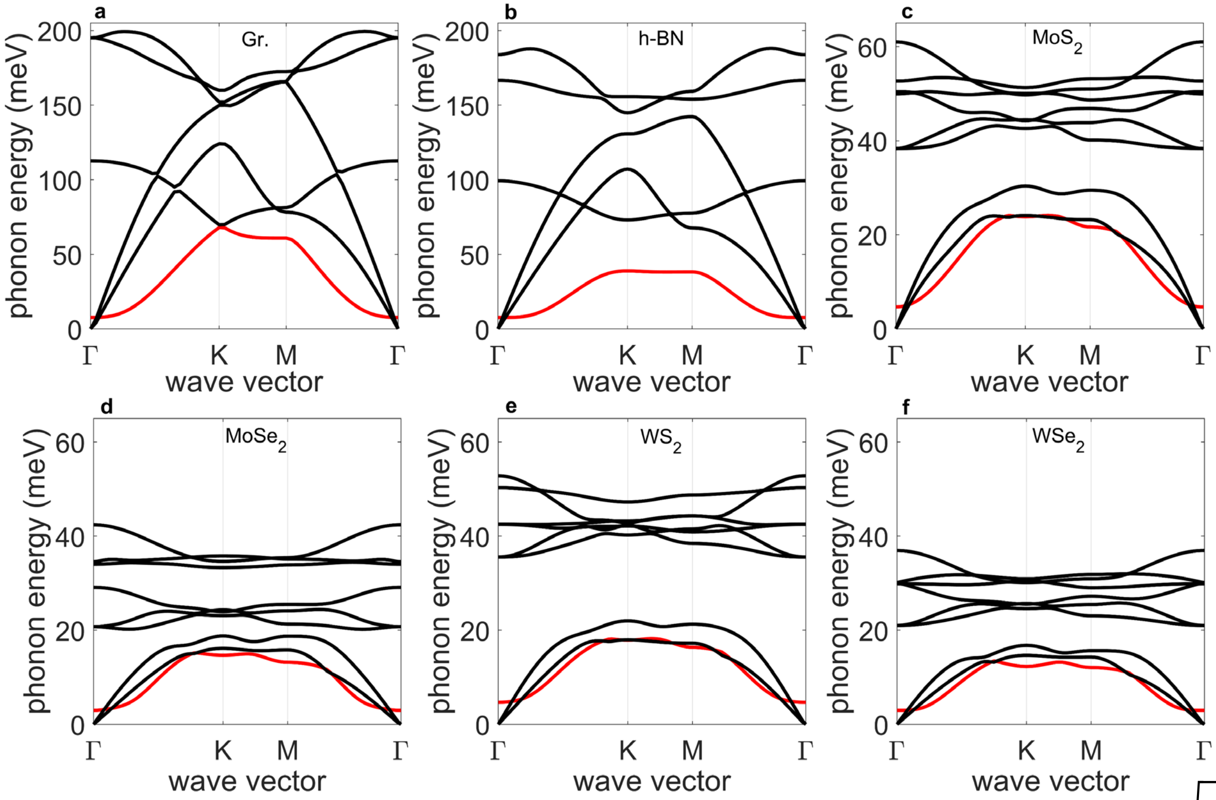

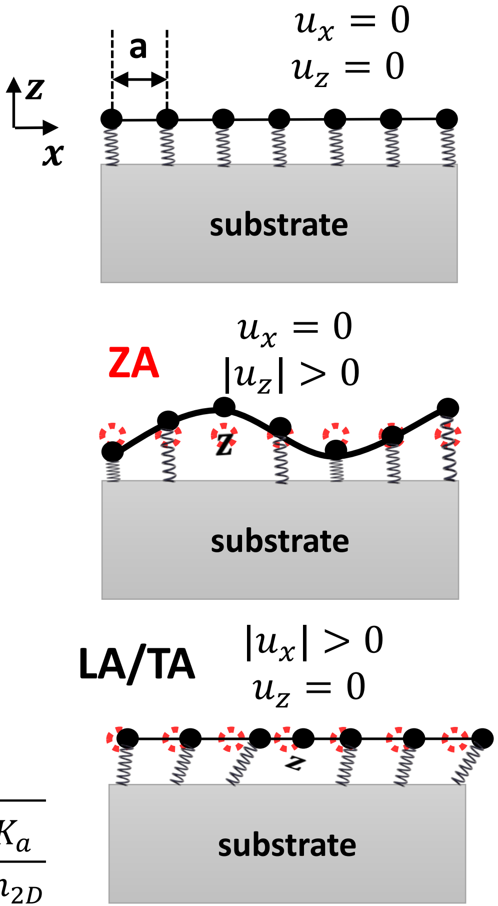

$$\tilde{\omega}_{ZA} = \sqrt{\omega_{ZA}^2 + \omega_0^2} \qquad \omega_0 = \sqrt{\frac{K_a}{m_{2D}}}$$

Foss and Aksamija, 2D Mater. 6 (2019) 025019

Temperature dependent TBC

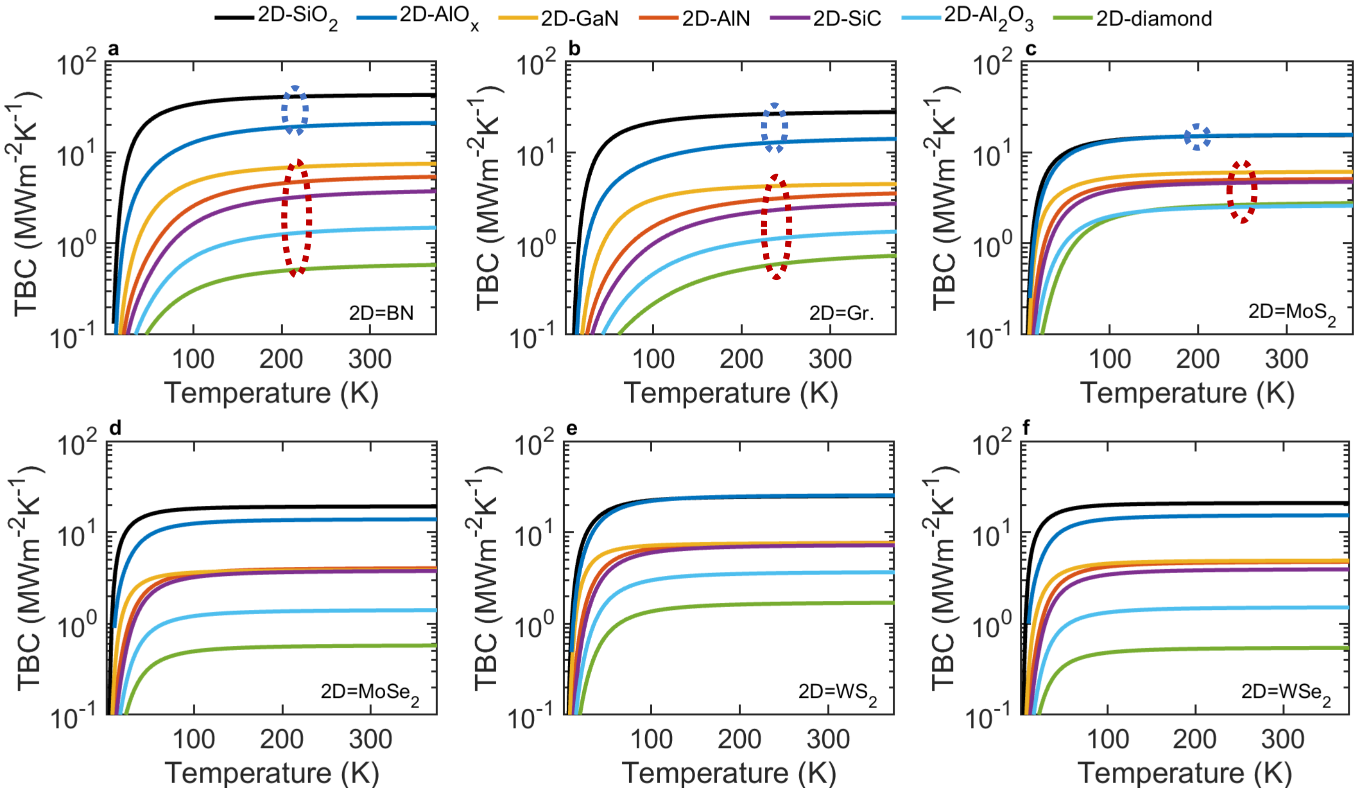

Assuming the same coupling (K_a) throughout:

2D materials on amorphous substrates consistently show higher TBC than crystalline substrates.

Foss and Aksamija, 2D Mater. 6 (2019) 025019

Phonon Density of States (DOS)

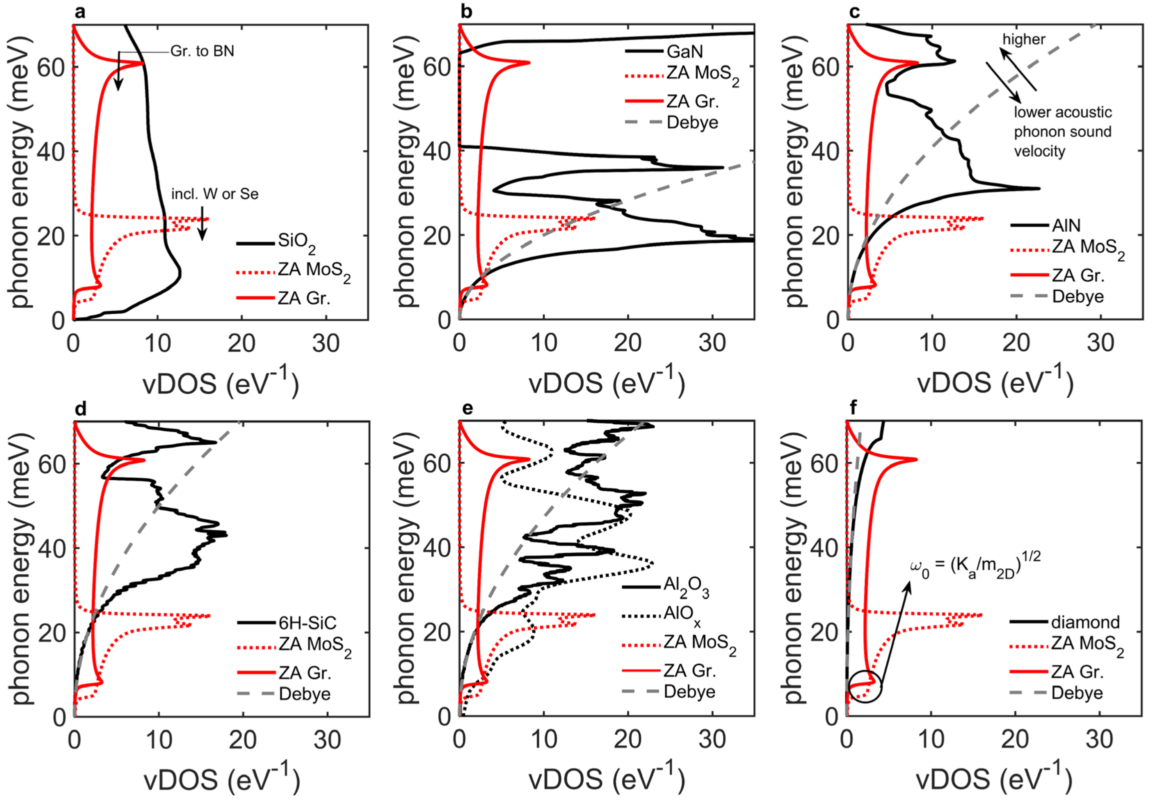

DOS of crystalline materials follows the **Debye model** at low energies

$$D_{sub}(\omega) = 3\frac{\omega^2}{2\pi^2 v_{sub}^3}$$

Amorphous materials deviate from the Debye model due to the randomization of atomic positions.

Leading to a large peak in the DOS of amorphous materials, often termed the **Boson Peak**.

Recall, $\Gamma_{sub}(\omega) \propto \frac{1}{\omega^2}$

Foss and Aksamija, 2D Mater. 6 (2019) 025019

Correlation between TBC and material properties

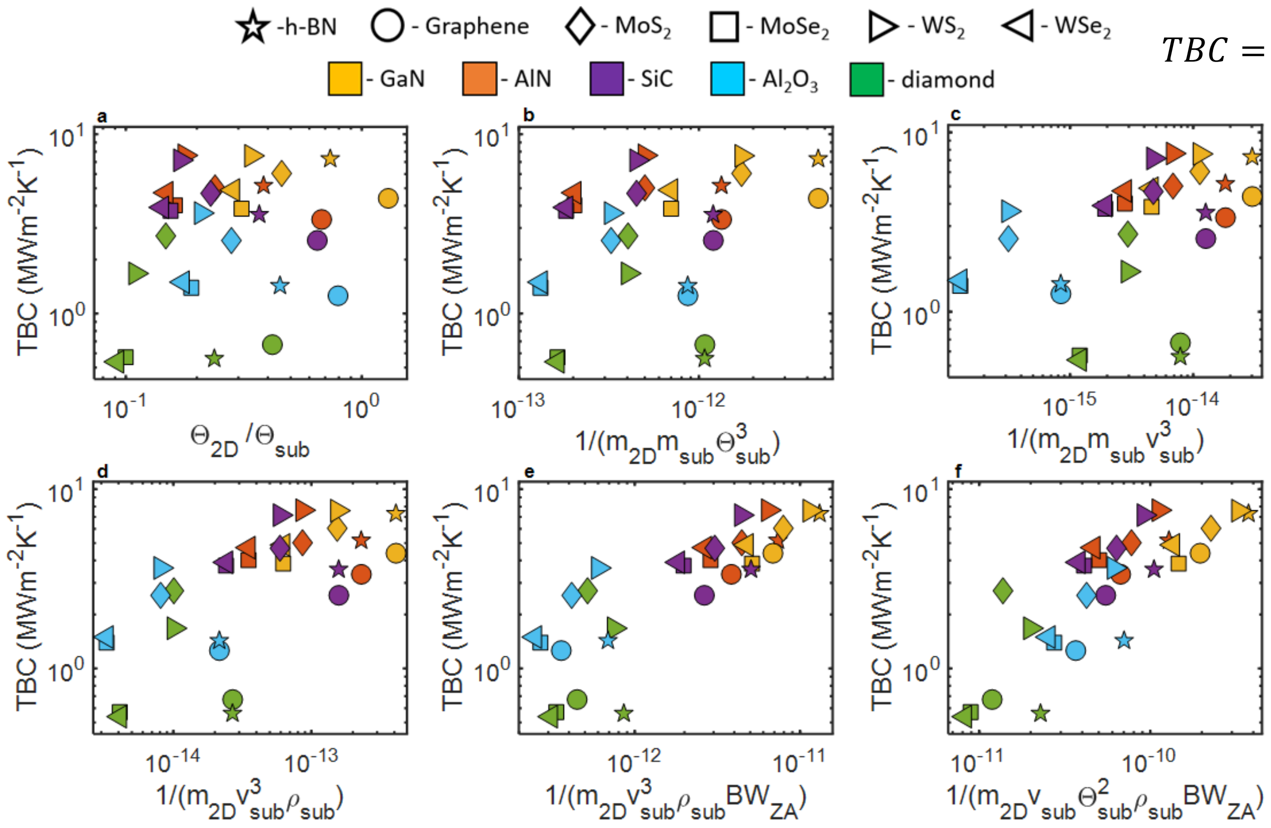

$$TBC = G(T) = \int C_{2D}(\omega,T) D_{2D}(\omega) \Gamma_{sub}(\omega) d\omega$$

$$\Gamma_{sub}(\omega) = \frac{\pi}{2} \frac{D_{sub}(\omega)}{m_{sub} m_{2D}} \frac{K_a^2}{\omega^2}$$

Debye model for substrate DOS:

$$D_{sub}(\omega) = 3 \frac{\omega^2}{2\pi^2 v_{sub}^3}$$

$$\Gamma_{sub}(\omega) = \frac{3}{4\pi} \frac{K_a^2}{m_{2D} m_{sub} v_{sub}^3}$$

Analytical approximations:

$$\tilde{G}_1(T) \approx \frac{3}{4\pi} \frac{K_a^2}{m_{2D} m_{sub} v_{sub}^3} C_{2D}^v(T)$$

$$\tilde{G}_2(T) \approx \frac{1}{4\pi} \frac{K_a^2}{m_{2D} v_{sub}^3 \rho_{sub}} C_{2D}^v(T)$$

Foss and Aksamija, 2D Mater. 6 (2019) 025019

@ 300K

TBC as a function of Boson Peak location

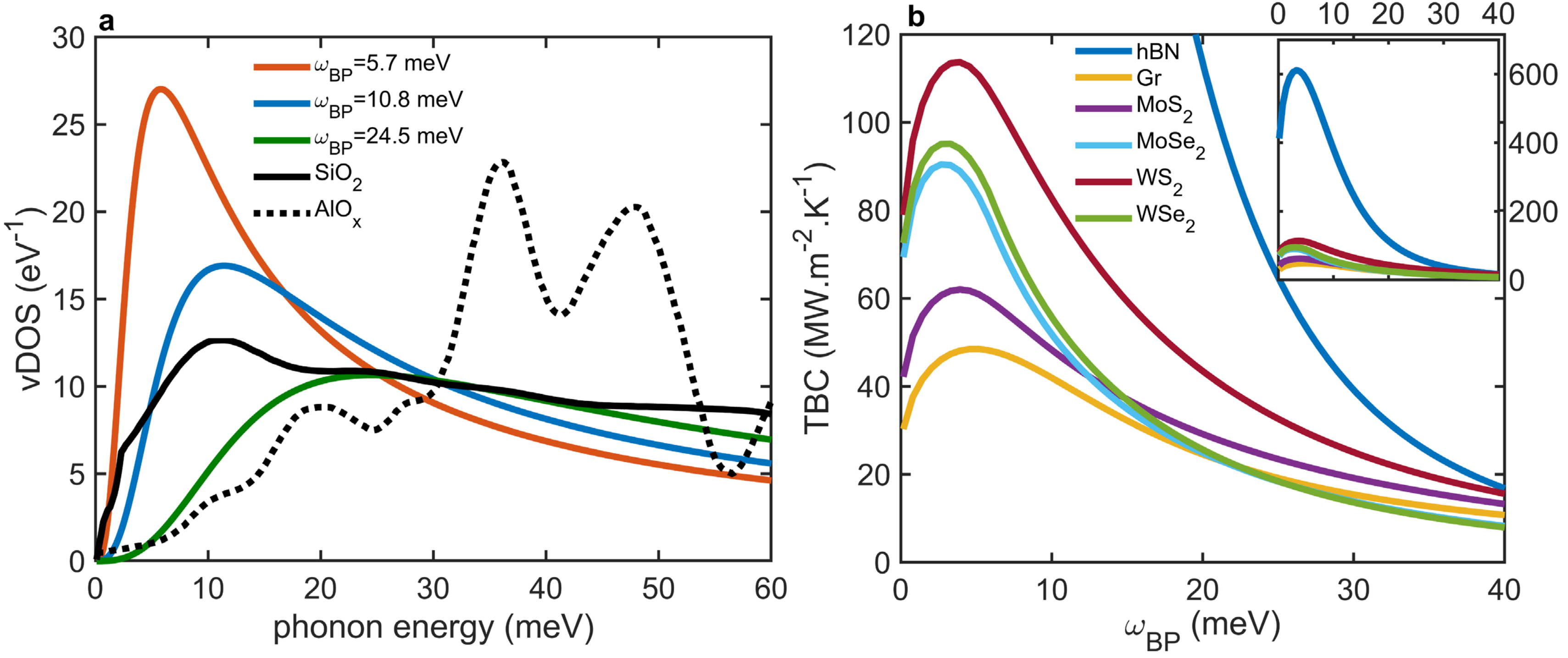

Lorentzian squared function: $D_{BP}(\omega) = \frac{\omega^3}{(\omega^2 - v_0^2)^2}$ $\qquad \omega_{BP} = \sqrt{3}v_0$

Foss and Aksamija, 2D Mater. 6 (2019) 025019

Conclusion (pt. 2)

- **Amorphous substrates enable better heat transfer across a 2D-3D interface** due to their large DOS near low energies (Boson Peak) which maximizes $\Gamma_{sub} \propto \frac{1}{\omega^2}$.
- **There is a tradeoff between improved 2D/3D TBC and thermal conductivity of the substrate**
  - Amorphous: good TBC, poor κ
  - Crystalline: poor TBC, (typically) good κ
- **hBN demonstrates superior TBC than our other tested 2D-layers** due to its light atomic mass and flatter ZA branch dispersion.
- The TBC between 2D-materials and crystalline substrates strongly follows the inverse of the product of:
  - Atomic mass of the 2D-layer
  - Sound velocity of the substrate
  - Mass density of the substrate
  - Debye temperature of the substrate squared
  - Phonon bandwidth of the ZA branch of the 2D material

i.e., for 2D materials on crystal substrates $\mathbf{TBC} \propto \frac{\mathbf{1}}{m_{2D} v_{sub} \Theta_{sub}^2 \rho_{sub} BW_{ZA}}$.

Acknowledgement: this work was supported by the National Science Foundation Emerging Frontiers in Research and Innovation (EFRI) grant

Questions?

UMassAmherst
The Commonwealth's Flagship Campus

Electrical transport in a CVD-grown graphene

UMassAmherst

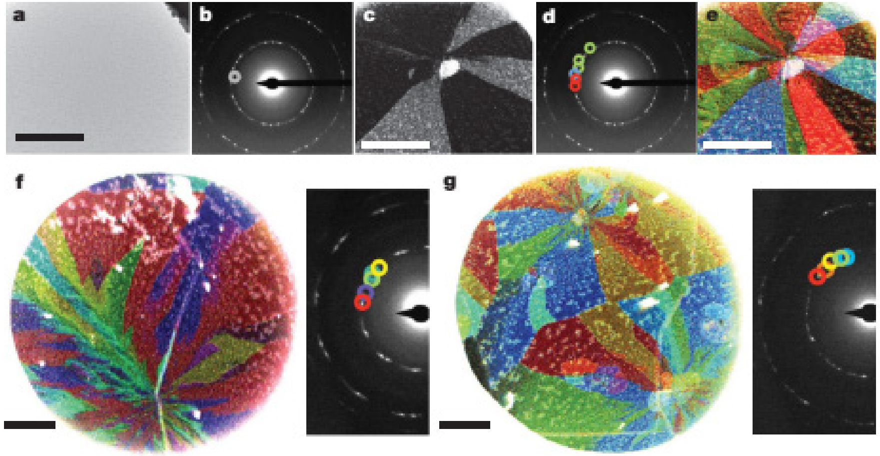

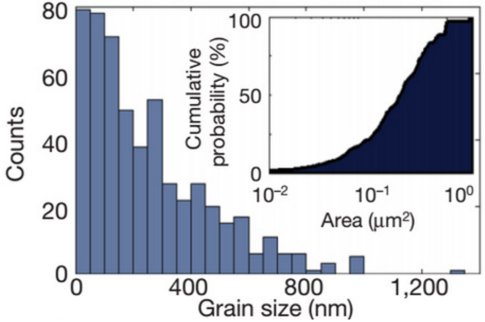

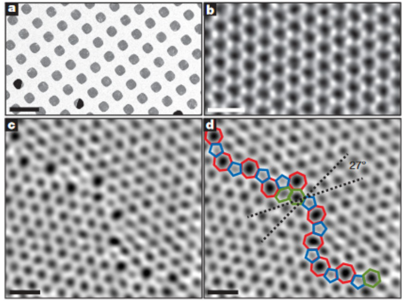

Huang et al., Nature 09718, Vol 469 (2011) 389–393

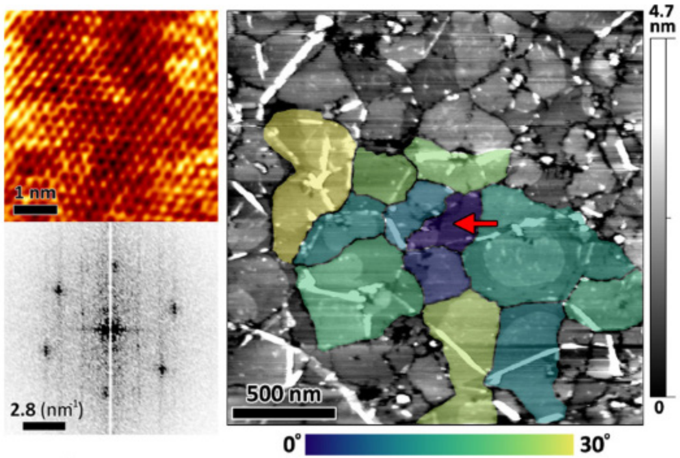

Nemes-Incze et al., Appl. Phys. Lett. 99, (2011), 023104

Resistivity across a single GB varies from 10^2 to 10^{15} $\Omega\ \mu m$. How does a CVD-grown graphene sheet conduct electricity?

Literature on graphene GB resistance

g

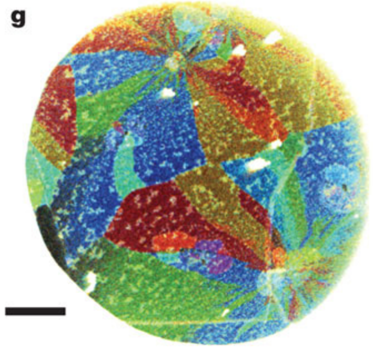

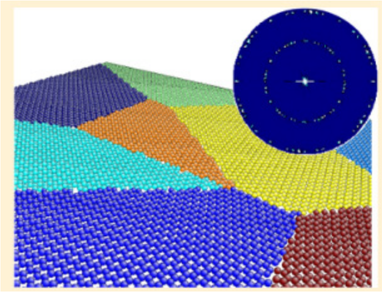

Liu et al., J. Phys. Chem. C, 2014

Huang et al., Nature 469, 2011

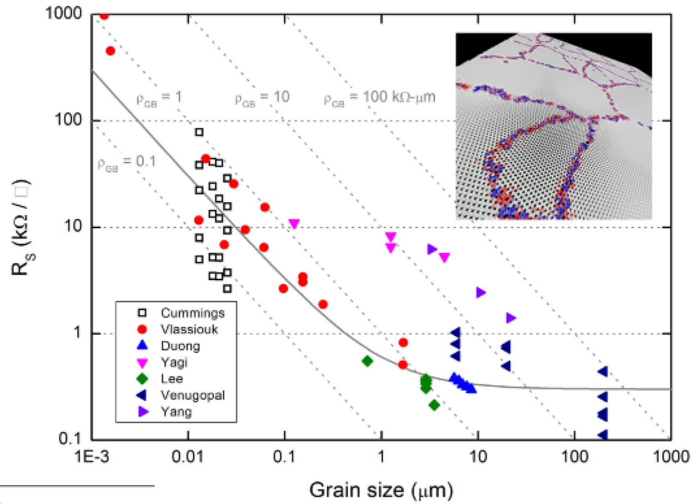

Isacsson et al., 2D Mater. 4 (2016), 012002

Device or study	ρ_{GB} (Ω μm)	Measurement	Fabrication/grain notes
Device 2 (Fig. S4)	8 ± 8	This study	Electropolished Cu, APCVD, hexagonal grains
Device 1 (Fig. 3)	120 ± 60		
Device 3 (Fig. S5)	150 ± 30		
Huang[11]	<60	AC-EFM	LPCVD, dendritic/Flower patchwork grains
Clark[12]	43–140	4-Probe STM	Electropolished Cu
			APCVD, hexagonal grains
Tsen[13]	650–3200	Resistive	LPCVD (2 Torr)
			Patchwork grains
	12 900–43 000	Resistive	Formed Cu pocket,[32]
			LPCVD (2 Torr), dendritic / flower grains
Yu[9]	8400	Resistive	APCVD, hexagonal grains
Jauregui[10]	2000–15 000	Resistive	APCVD, hexagonal grains

Grosse et al., Appl. Phys. Lett. 105, 2014

Mimicking CVD-grown graphene via Voronoi diagrams

UMassAmherst

CVD-grown graphene

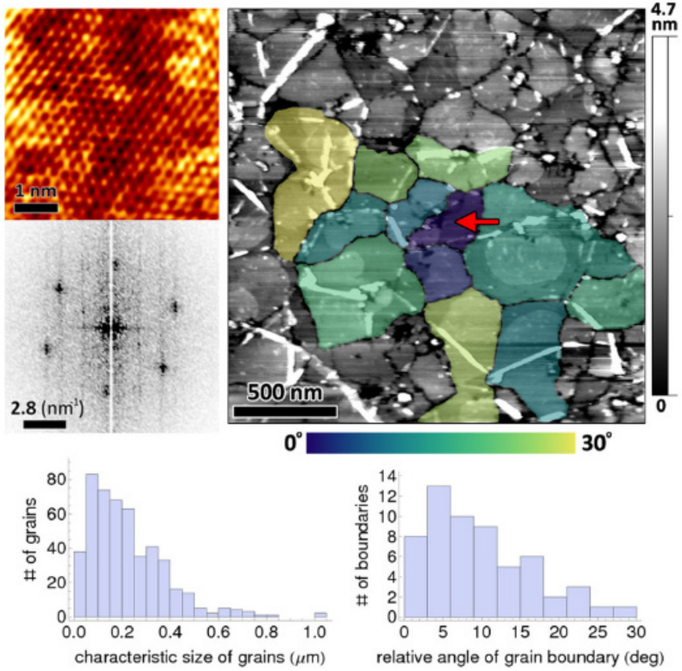

Nemes-Incze et al., Appli. Phys. Lett. 99, (2011), 023104

Simulating CVD graphene

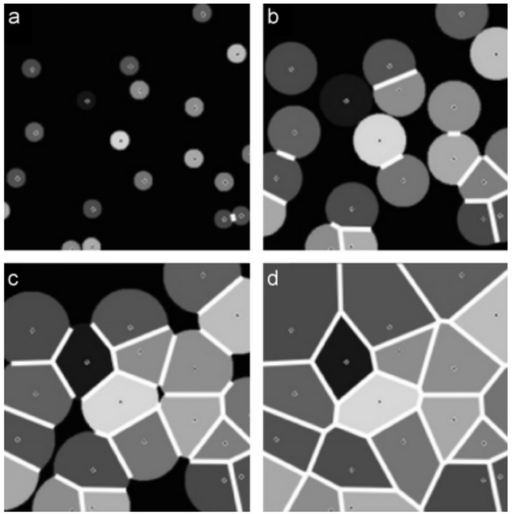

Avrami-Johnson-Mehl method

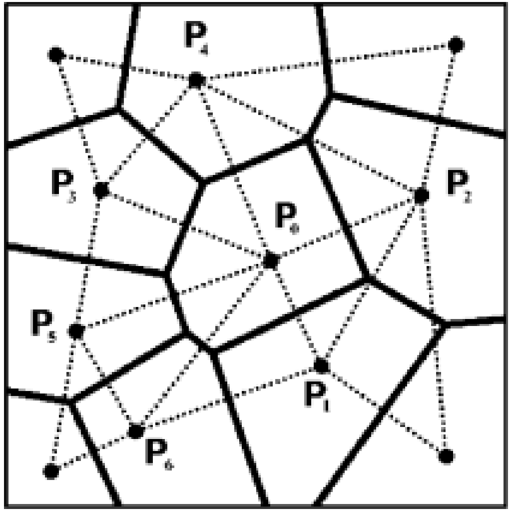

Perpendicular bisector method

Ferenc et al., Physica A 385 (2007), 518–526

Simulation set-up to calculate thermal conductivity

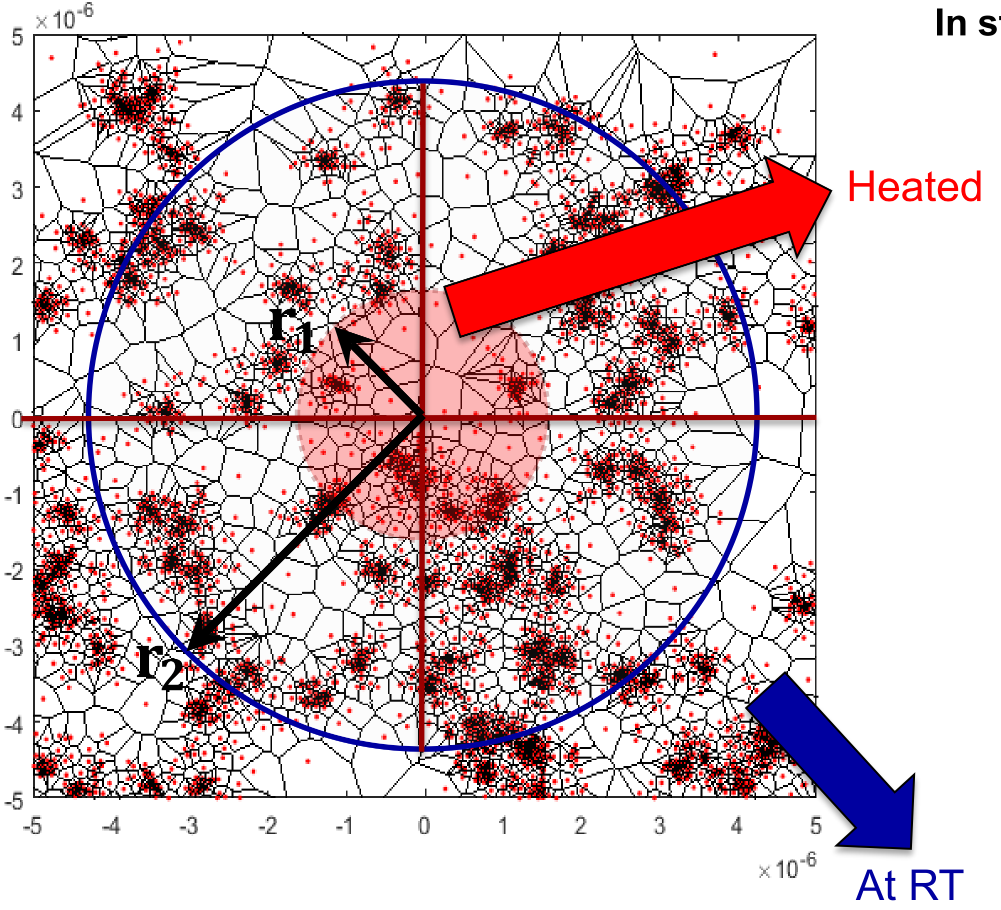

In steady state, the net heat flux through the GB=0

$$\sum_j G_{ij}(T_i - T_j) + S_i Q_i = 0$$

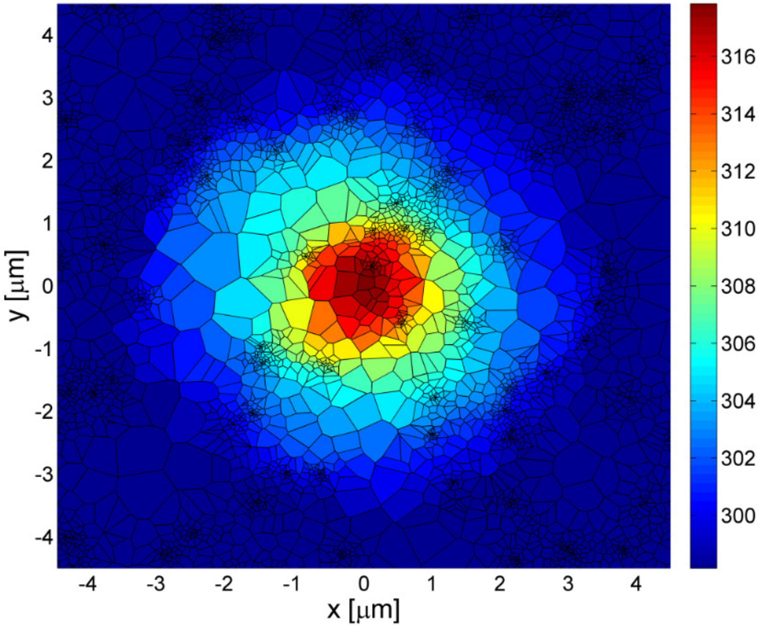

Temperature profile at steady state condition

Aksamija and Knezevic, PRB 90, (2014), 035419

Adapting the model for electron transport

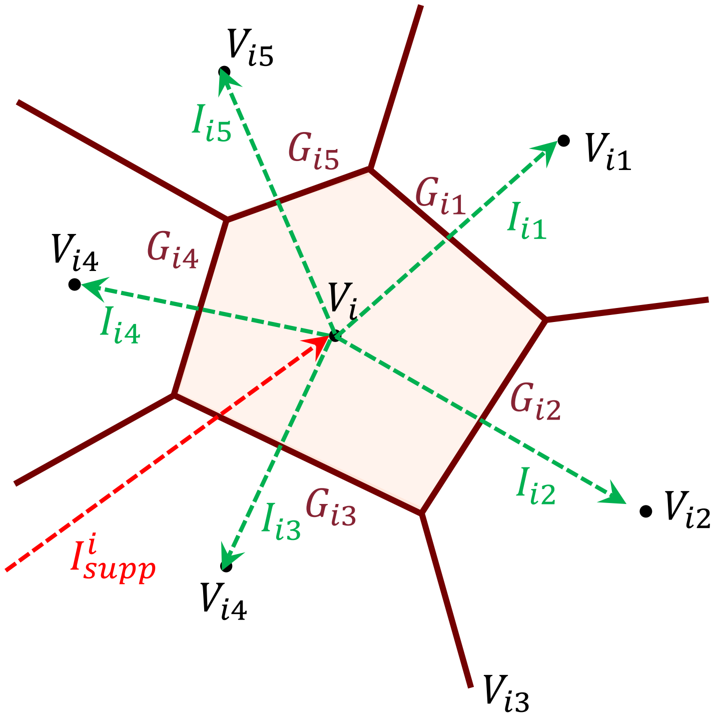

G_{ij} comprises of grain resistance and GB resistance due to mismatch angle.

In steady state, the net current through the GB=0

$$\sum_j I_{ji} + I^i_{supp} = 0$$

$$\sum_j (V_i - V_j) G_{ij} + I^i_{supp} = 0$$

Solve for potential of each grain iteratively

$$V_i^{n+1} = \frac{G_{ij} V_i^n + I_{supp,i}}{G_{ij}}$$

Until $\Delta V_i = \left| \frac{V_i^{n+1} - V_i^n}{V_i^{n+1}} \right| < tolerance$

for all the grains

Steady-state grain voltages and sheet conductance

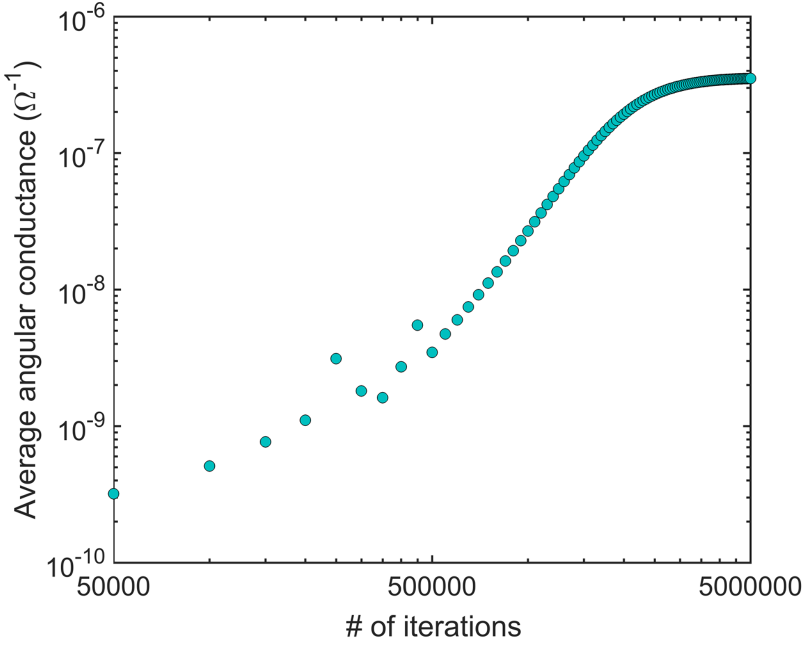

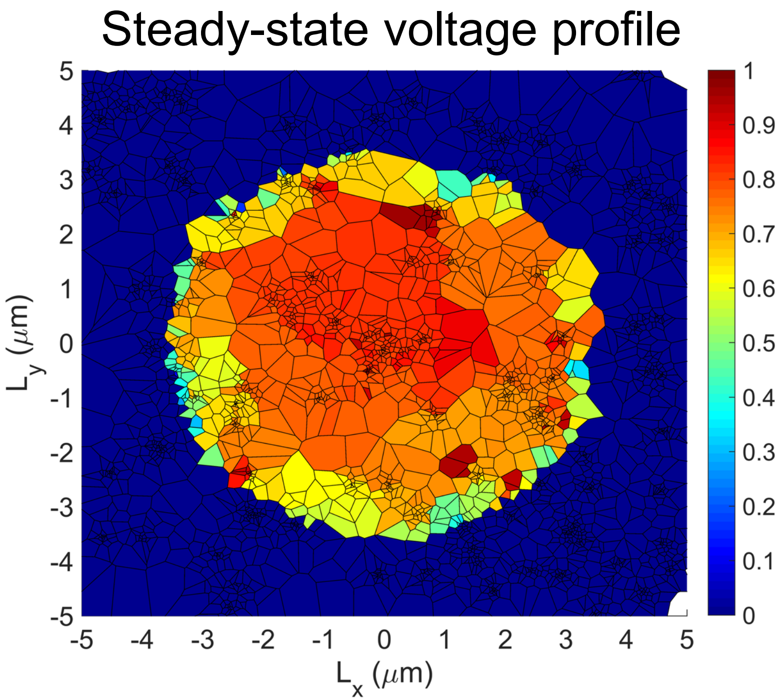

$$G(\Theta) = \frac{\sum_j I_{supp}^{j}}{[V_{in}(\Theta) - V_{out}(\Theta)]} \frac{ln(r_{out}/r_{in})}{2\pi}$$

Average steady-state conductance=$3.5 \times 10^{-7}\ \Omega^{-1}$

Angular conductance is

$$G(\Theta) = \frac{\sum_j I_{supp}^j}{[V_{in}(\Theta) - V_{out}(\Theta)]} \frac{ln(r_{out}/r_{in})}{2\pi}$$

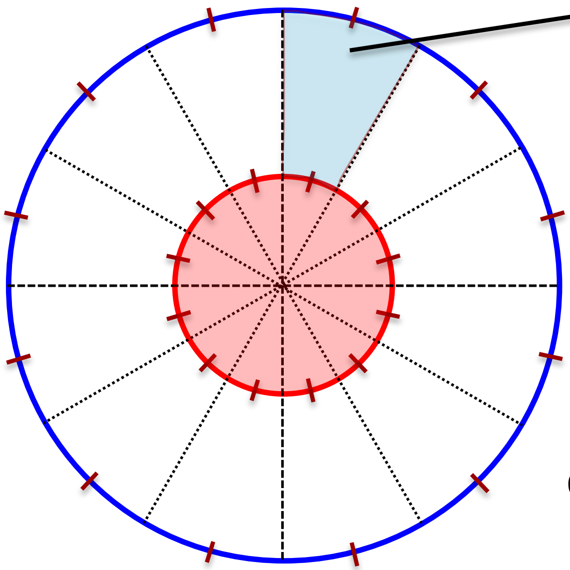

$$A^i = \pi(r_{out}^2 - r_{in}^2)/n$$

$$W_{eff}^i = \frac{A^i}{L_{eff}} = \frac{\pi(r_{out} + r_{in})}{n}$$

$$G_{sheet} = \sum_i G_{sheet}^i$$

$$G_{sheet}^i = G^i \frac{W_{eff}^i}{L_{eff}} = G^i \frac{\pi(r_{out}+r_{in})}{(r_{out}-r_{in})n},$$

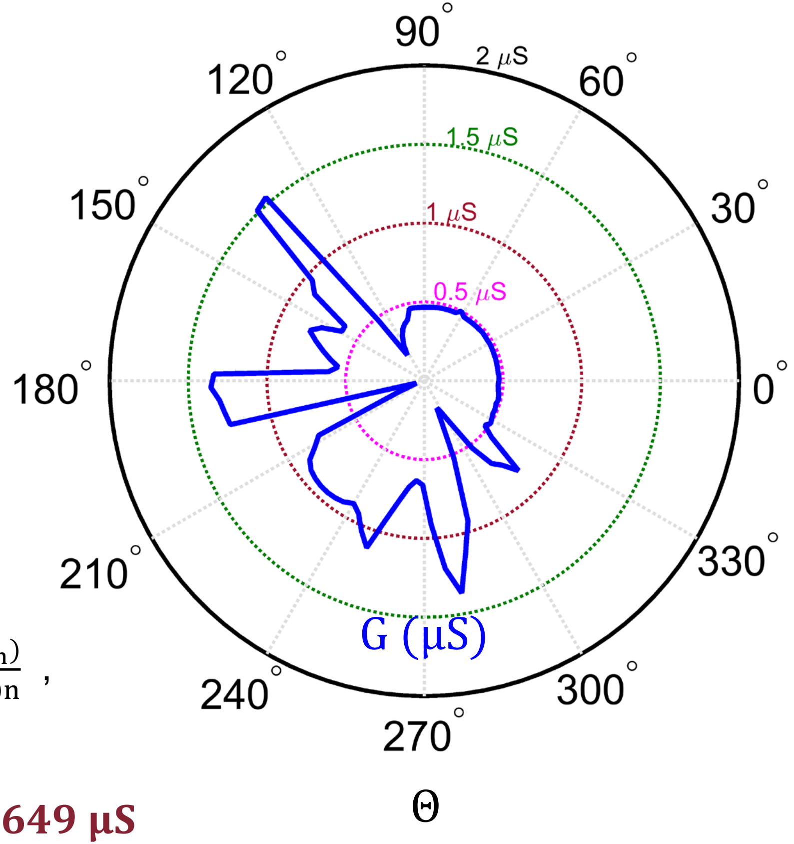

Average conductance is $0.649\ \mu S$

Constructing non-straight Grain boundaries

UMassAmherst

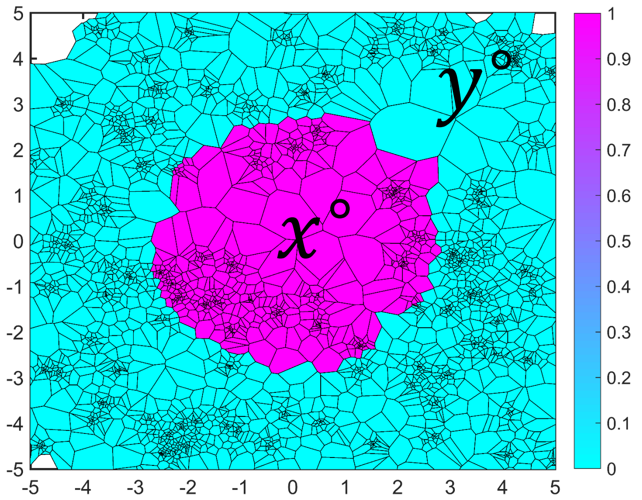

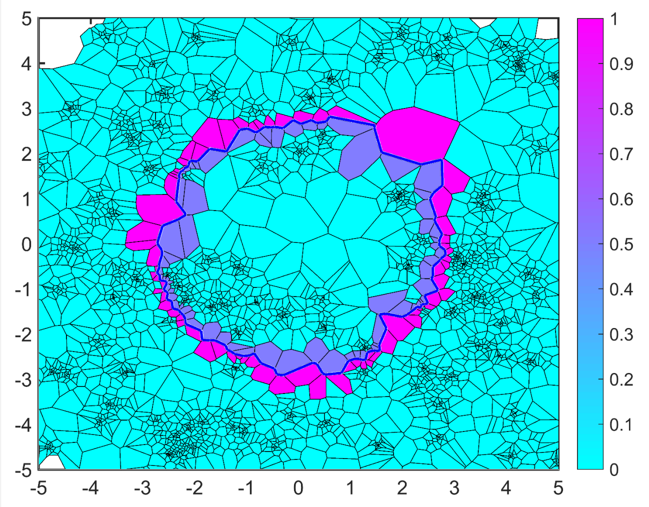

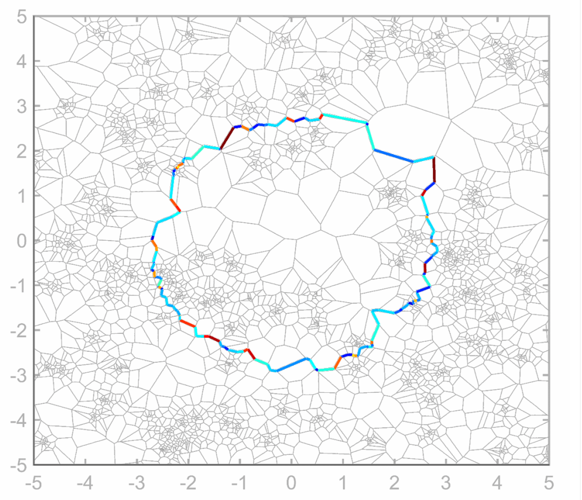

Grains boundaries are seldom straight lines

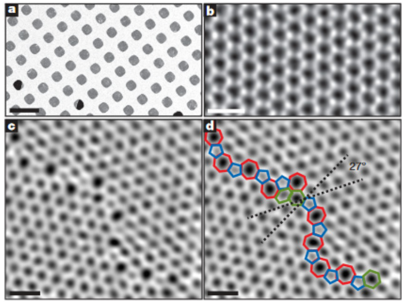

Huang et al., Nature 09718, Vol 469 (2011) 389–393

Linear colormap showing GB resistance of each segment of the GB.

Effective resistivity of “rough” GBs

Despite local GB resistivity being very high (Gohms), the effective resistivity of non-straight GBs is far lower (1-10 kOhm)

Variation due to randomly generated GBs

Possible impact on variability of devices or interconnect made from CVD-grown material